Discovery of Pyrrolopyridine−Pyridone Based Inhibitors of Met Kinase: Synthesis, X-ray Crystallographic Analysis, and Biological Activities

Kyoung Soon Kim,*[,†] Liping Zhang,[†] Robert Schmidt,[†] Zhen-Wei Cai,[†] Donna Wei,[†] David K. Williams,[†] Louis J. Lombardo,[†] George L. Trainor,[†] Dianlin Xie,[⊥] Yaquan Zhang,[⊥] Yongmi An,[⊥] John S. Sack,[⊥] John S. Tokarski,[⊥] Celia Darienzo,[§] Amrita Kamath,[§] Punit Marathe,[§] Yueping Zhang,[‡] Jonathan Lippy,[Δ] Robert Jeyaseelan, Sr.,[‡] Barri Wautlet,[‡] Benjamin Henley,[‡] Johnni Gullo-Brown,[‡] Veeraswamy Manne,[‡] John T. Hunt,[‡] Joseph Fargnoli,[‡] and Robert M. Borzilleri[†]

Departments of Oncology Chemistry, Oncology Drug Discovery, Structural Biology and Modeling, and Metabolism and Pharmacokinetics, Bristol-Myers Squibb Pharmaceutical Research & Development, P.O. Box 4000, Princeton, New Jersey 08543-4000

Received April 24, 2008

Conformationally constrained 2-pyridone analogue **2** is a potent Met kinase inhibitor with an IC_{50} value of 1.8 nM. Further SAR of the 2-pyridone based inhibitors of Met kinase led to potent 4-pyridone and pyridine *N*-oxide inhibitors such as **3** and **4**. The X-ray crystallographic data of the inhibitor **2** bound to the ATP binding site of Met kinase protein provided insight into the binding modes of these inhibitors, and the SAR of this series of analogues was rationalized. Many of these analogues showed potent antiproliferative activities against the Met dependent GTL-16 gastric carcinoma cell line. Compound **2** also inhibited Flt-3 and VEGFR-2 kinases with IC_{50} values of 4 and 27 nM, respectively. It possesses a favorable pharmacokinetic profile in mice and demonstrates significant in vivo antitumor activity in the GTL-16 human gastric carcinoma xenograft model.

Introduction

The Met receptor tyrosine kinase is a transmembrane growth factor receptor that plays a critical role in both normal development and tumorigenesis.[1] The disulfide-linked heterodimeric Met protein consists of an α- and β-subunit with the receptor tyrosine kinase domain residing in the β-chain. Met is expressed predominantly on epithelial and endothelial cells. It mediates a variety of epithelial functions, and deregulation of the HGF/Met pathway has been implicated in a wide variety of malignancies.[2] Upon binding to its ligand, hepatcyte growth factor (HGF), also known as scatter factor (SF), Met autophosphorylates tyrosines 1234 and 1235 within the activation loop (A-loop).

Subsequently, phosphorylation of Y1349 and Y1356 in the multifunctional docking site at the C terminus occurs, which mediates the docking of multiple downstream signal transducers such as PI3K, SRC, and SHC.[1,3,4] The biological consequences of HGF/Met signal transduction include tumor growth, induction of cell motility, invasiveness, metastases, and angiogenesis.[1] Overexpression of Met or HGF and/or amplification of the Met gene is frequently observed in a variety of human tumors including liver, breast, pancreas, lung, kidney, bladder, ovary, brain, prostate, and myeloma, among others.[5,6] The HGF/Met signaling pathway has been a popular target for diagnosis and therapeutic intervention of human cancer. The growing list of experimental reagents with therapeutic potential that target the HGF/Met signaling pathway includes small molecules as well as various biologicals that include neutralizing antibodies against human HGF/SF and Met.[7,8]

The pyrrolopyridine derivative **1**, containing an acylurea moiety, was previously reported to have potent Met kinase inhibitory activity (Figure 1).[9] Replacement of the acylurea moiety by a conformationally constrained 2-pyridone as in analogue **2** was envisioned as a new Met kinase inhibitor chemotype (Figure 2). Structure−activity relationship (SAR) studies on the 2-pyridone analogues led to the identification of 4-pyridone **3** and pyridine *N*-oxide **4** (Figure 2). The synthesis, SAR, structural biology, and in vivo biological activities of these compounds are described.

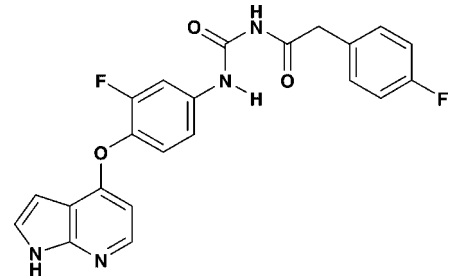

Figure 1. Pyrrolopyridine *N*-acylurea **1**.

Chemistry

Aminophenoxypyrrolopyridine **8** was prepared by coupling 4-chloropyrrolopyridine **5**[10] with 2-fluoro-4-nitrophenol **6**, followed by reduction of the nitro group of intermediate **7** using zinc metal (Scheme 1). Michael addition of 4-fluoroaniline **10** to pyrone ester **9** followed by intramolecular cyclization of the Michael adduct provided *p*-fluorophenyl-2-pyridone ester **11**, which was hydrolyzed to afford *p*-fluorophenyl-2-pyridone acid **12**. Coupling of amine **8** with 2-pyridone acid **12** produced pyrrolopyridine-2-pyridone analogue **2**. 2-Pyridone analogues **13**−**20** (Table 1) were synthesized using similar procedures illustrated in Scheme 1.

The syntheses of various 4-pyridone substituted analogues are depicted in Schemes 2−4. Fluorophenyl-β-keoester **24**, which was prepared from Meldrum's acid adduct **23** according to the literature procedure,[11] was reacted with triazine **25** to obtain ester **26**.[12] Ester **26** was hydrolyzed to yield 3-fluorophe-

* To whom correspondence should be addressed. Phone: (609) 252-5181. Fax: (609) 252-6601. E-mail: kyoung.kim@bms.com.
[†] Department of Oncology Chemistry.
[⊥] Department of Structural Biology and Modeling.
[§] Department of Metabolism and Pharmacokinetics.
[‡] Department of Discovery Biology.
[Δ] Department of Lead Evaluation.

10.1021/jm800476q CCC: $40.75
Published on Web 08/09/2008

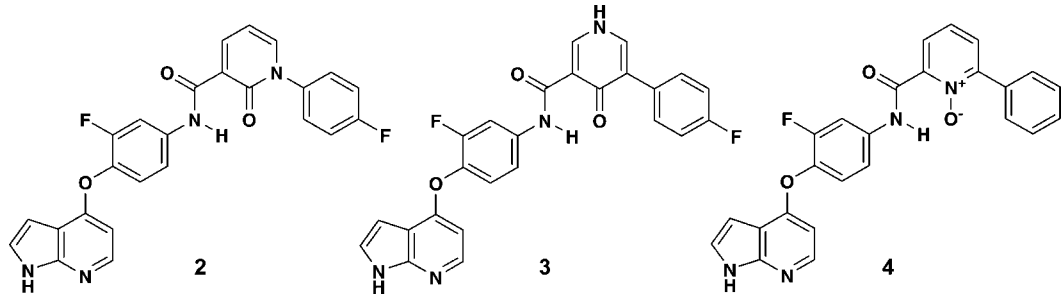

Figure 2. 2-Pyridone, 4-pyridone, and pyridine *N*-oxide inhibitors.

Scheme 1[a]

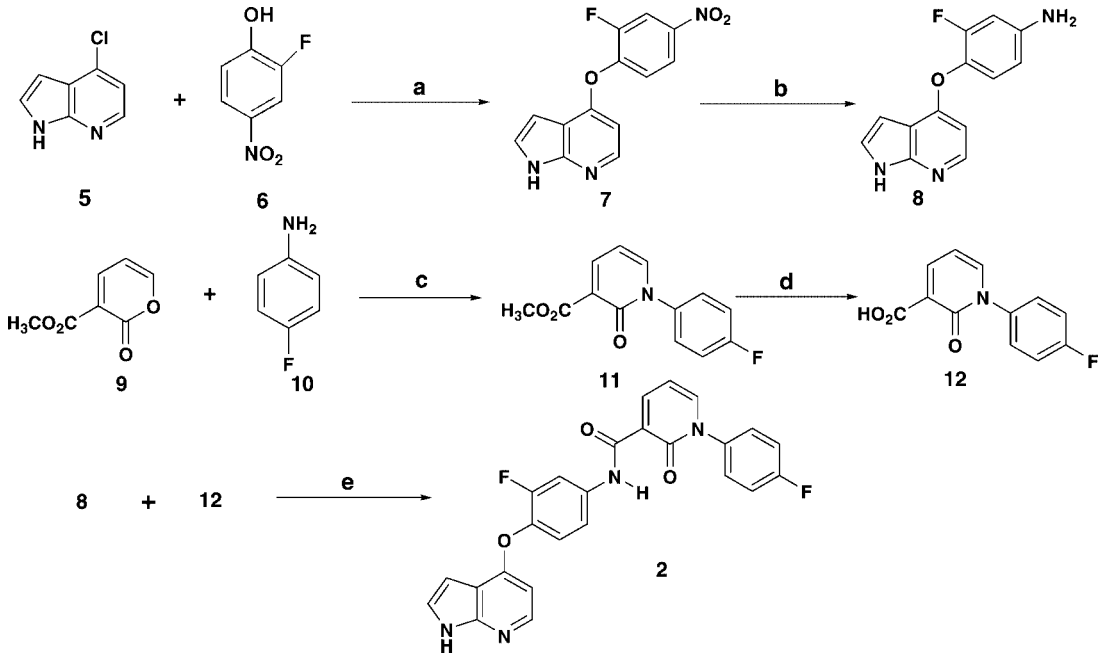

[a] Reagents and conditions: (a) *i*-Pr_2NEt, microwave, 200 °C, NMP, 43%; (b) Zn, NH_4Cl, MeOH/THF, room temp, overnight, 77%; (c) DMF, 0 °C, 7 h; EDCI, DMAP, room temp, overnight, 64%; (d) 2 N NaOH, MeOH, 65 °C, 1.5 h, 99%; (e) TBTU, DMF/CH_3CN, 0 °C to room temp, 3 h, 81%.

nylpyridine-4-pyridone acid **27**. Coupling of acid **27** with pyrrolopyridine amine **8** provided 4-pyridone analogue **3** (Scheme 2). *N*-Methyl or *N*-hydroxyethyl substituted 4-pyridone analogues **34** and **37** were obtained from intermediate 3-bromo-4-hydroxypyrine-5-carboxylic acid **29**, which was obtained from 3,5-dibromo-4-hydroxypyridine **28**[13] via metalation and carboxylation (Scheme 3). Alkylation of acid **29** with methyl iodide or the methyl ester of **29** with 2-hydroxybromoethane yielded N-substituted 4-pyridone esters **30** and **35**, respectively. Miyaura−Suzuki coupling reaction[14] of the bromo-4-pyridone esters **30** and **35** with *p*-fluorophenylboronic acid, followed by hydrolysis to the corresponding acids, and coupling of the acids **33** and **36** with pyrrolopyridine amine **8** afforded N-substituted 4-pyridone analogues **34** and **37**, respectively. Alternatively, N-substituted 4-pyridone analogues **41**−**43** were prepared directly from 4-oxopyran **40** using the corresponding amine or aniline (Scheme 4). Pyrone aldehyde **38**,[15] which was obtained by Vilsmeier−Haack reaction of 4-fluorophenylacetone, was oxidized and converted to the acyl chloride **39**. Coupling between acyl chloride **39** and pyrrolopyridine amine **8** afforded 4-pyrone **40**. Reaction of pyrone **40** with various amines provided N-substituted 4-pyridone analogues **41**−**43**.

The synthesis of pyridine and pyridine *N*-oxide analogues **47** and **4** are described in Scheme 5. Phenylpicolinic acid **45** and 6-phenylpicoloinic acid *N*-oxide **46** were obtained by Miyaura−Suzuki coupling of 2-bromopicolinic acid **44** with phenylboronic acid followed by oxidation. Coupling of 6-phenylpicoloinic acid **45** or 6-phenylpicoloinic acid *N*-oxide **46** with pyrrolopyridine amine **8** produced pyridine analogue **47** and pyridine *N*-oxide **4**.

Structure−Activity Relationships and Structural Studies

2-Pyridone analogues with hydrophobic phenyl substituents **2** and **13** (Table 1) displayed potent Met kinase inhibitory activities with IC_{50} values in the single digit nanomolar range. An X-ray crystal structure of **2** bound to the Met kinase domain revealed that it binds to the ATP-binding pocket of the Met protein in an inactive conformation; i.e., the activation loop folds back toward the ATP-binding pocket (Figure 3).[16] The DFG motif, which is conserved among kinases and marks the beginning of the activation loop, is observed in the structure, but most of the remaining loop is undefined. The N1 nitrogen of the pyrrolopyridine ring engages in hydrogen bonding with the backbone NH of Met1160 of the hinge region, and the NH of the pyrrolopyridine ring hydrogen-bonds with the Met1160 carbonyl oxygen. The central aminophenyl ring is flanked on one side by the gatekeeper residue Leu1157 and on the opposite face by the side chain of Phe1223 (of the DFG motif) in a face-to-face aromatic interaction. The 2-pyridone carbonyl oxygen hydrogen-bonds with the backbone NH of Asp1222. The 4-fluorophenyl ring lies in a hydrophobic pocket comprising Phe1134, Phe1200, Met1131, and Leu1195. Replacement of the

Scheme 2[a]

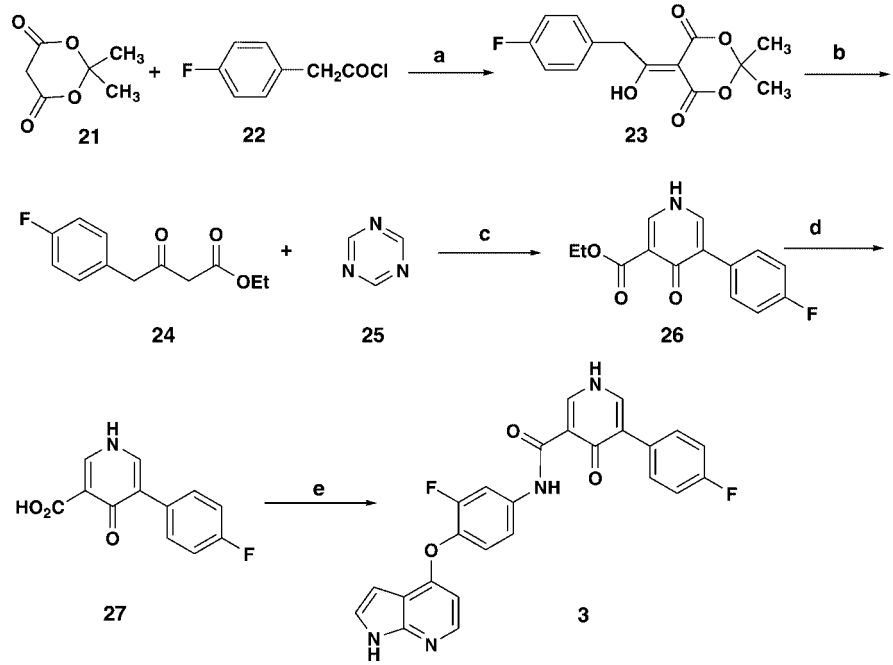

[a] Reagents and conditions: (a) pyridine, CH_2Cl_2, 0 °C, 2.5 h; (b) EtOH, reflux, 16 h, 48% overall; (c) NaOEt, EtOH, room temp, 2 h, 78%; (d) 2 N NaOH, MeOH, 97%; (e) **8**, HATU, *i*-Pr_2NEt, DMF, 0 °C to room temp, 40%.

Table 1. SAR of 2-Pyridone Analogues

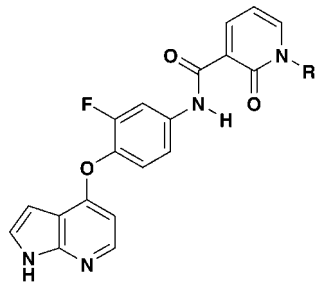

		IC_{50} (nM)		
compd	R	Met (biochemical)	GTL-16 (cellular)	N87 (cellular)
2	*p*-F-phenyl	1.8 ± 0.7	60	>5000
13	C_6H_5	1.9 ± 0.1	140	>5000
14	*tert*-butyl	1000 ± 0.0	NT	NT
15	cyclopropyl	1000 ± 0.0	NT	NT
16	$CH_2CH_2CH(CH_3)_2$	30 ± 6.4	3700	>5000
17	*p*-F-benzyl	8.2 ± 1.4	2100	>5000
18	2-pyridyl	10 ± 0.7	970	>5000
19	3-pyridyl	70 ± 0.0	4000	>5000
20	C_6H_4-*p*-$CONH_2$	1000 ± 0.0	>5000	NT

terminal phenyl ring by *tert*-butyl or cyclopropyl (**14**, **15**) significantly reduced the kinase inhibitory activitiy, perhaps because both the *tert*-butyl and cyclopropyl groups are not sufficiently large enough to fill the hydrophobic pocket or lack the aromaticity to engage in π-electron interactions with the aromatic residues comprising the pocket. Interestingly, the larger alkyl isopentyl substituted analogue **16** restores most of the inhibitory activity. The weaker activity of the fluorobenzyl **17** compared to the fluorophenyl analogue suggests that the phenyl ring without a methylene linker is optimal for fitting into the hydrophobic pocket. Pyridyl substituted compounds (**18**, **19**) showed good activities, albeit weaker than the phenyl substituted analogues. The hydrophobic pocket does not appear to tolerate a polar substituent as seen with the poor activity of phenylcarboxamide **20**. However, the poor activity of **20** may alternatively be attributed to the fact that the pocket appears limited in size in the para-substituent direction.

The antiproliferative cellular activity of the Met inhibitors was evaluated in vitro using the GTL-16 gastric carcinoma cell line. GTL-16[17] is a subclone derived from MKN-45,[18] a poorly differentiated gastric carcinoma cell line carrying an amplification of the Met gene. The Met protein in the GTL-16 cell line is constitutively activated as observed by HGF ligand independent phosphorylation.[19,20] The GTL-16 cell line was previously shown to be highly sensitive to small molecule inhibitors of Met[20,21] and was adopted to be the primary in vitro cell line for screening Met inhibitors. In addition to these cell lines, inhibitors were routinely evaluated in the N87 gastric carcinoma cell line lacking Met activation.[22] Compounds **2** and **13** possess potent antiproliferative cellular activities against the GTL-16 gastric tumor cell line, while they lack cellular activity (IC_{50} > 5 μM) against the N87 cell line (Table 1). We believe the antiproliferative cellular activity difference in these two cell lines suggests that the Met receptor is the target of cellular growth inhibition.

As an extension of the 2-pyridone chemotype, 4-pyridone analogues (**3**, **34**, **37**, **41**−**43**, Table 2) were also prepared. The SAR of the 4-pyridones is consistent with predictions from the X-ray crystal structure of Met kinase bound to 2-pyridone analogue **2**, which reveals that the unsubstituted positions of the pyridinone ring are viable vectors for derivatization. The environment around the N-1 region of the 4-pyridinone ring is directed toward helix αC, which displayed mobility in its orientation in the X-ray structures (data not shown). The SAR revealed little difference in in vitro Met kinase inhibitory activity of analogues with N-1 substituents of different size and hydrophobicity (IC_{50} = 2.3−5.9 nM), which confirmed the flexibility of this region of the protein. All of these 4-pyridone analogues exhibit potent antiproliferative cellular activities

Scheme 3[a]

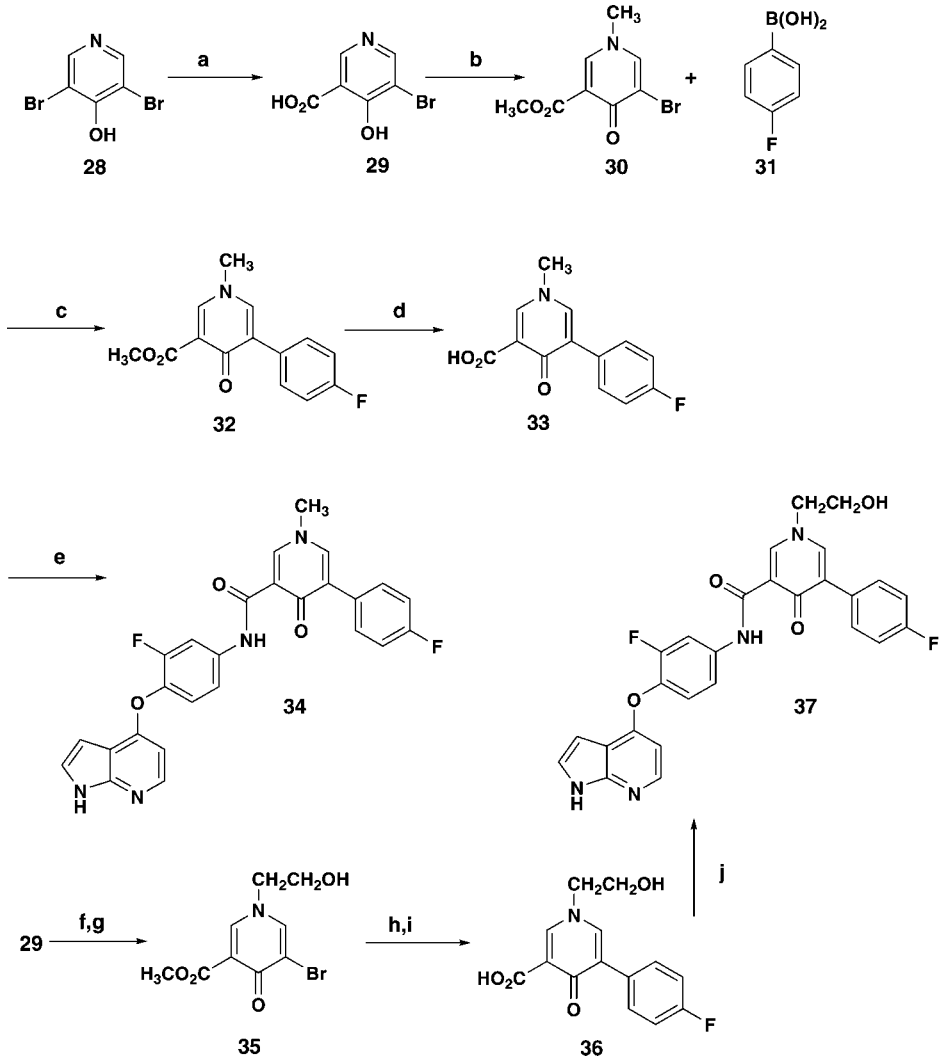

[a] Reagents and conditions: (a) MeLi, *n*-BuLi, CO_2, −78 °C, 85%; (b) CH_3I, Cs_2CO_3, DMF, room temp, 4 h, 86%; (c) $Pd(PPh_3)_4$, K_2CO_3, dioxane, 90 °C, 23 h, 21%; (d) 2 N NaOH, MeOH, 60 °C, 2 h, 86%; (e) **8**, HATU, *i*-Pr_2NEt, DMF, room temp, 1.5 h, 66%; (f) $SOCl_2$, MeOH, 0 to 70 °C, 93%; (g) $BrCH_2CH_2OH$, K_2CO_3, DMF, 50 °C, 87%; (h) **31**, $Pd(PPh_3)_4$, K_2CO_3, dioxane, 90 °C, 20 h, 22%; (i) 6 N NaOH, MeOH, room temp, 2 h, 89%; (j) **8,** HATU, *i*-Pr_2NEt, DMF, room temp, 1.5 h, 67%.

against the GTL-16 gastric tumor cell line with good selectivity over the N87 cell line.

Interestingly, pyrone **40** shows only weak activity despite its overall structural similarity. It is speculated that the vinylogous amide carbonyl in the 4-pyridone analogues makes it more basic and hence a better hydrogen bond acceptor than the carbonyl in pyrone **40**.

With the concept that the carbonyl oxygen of the pyridone analogues plays an important role in hydrogen-bonding with the backbone NH of Asp1222, the pyridine and pyridine *N*-oxide analogues were prepared (Table 3). Pyridine *N*-oxides **4** and**49** displayed potent Met kinase inhibitory activities with IC_{50} values of 1.3 and 1.8 nM, respectively, while pyridine analogue **47** showed much weaker inhibitory activity with an IC_{50} of 470 nM. Compounds **4** and **49** also possess potent antiproliferative cellular activities against GTL-16 with IC_{50} of 40 nM with good selectivity over the N87 cell line. Despite the presence of a basic pyridine nitrogen in **47**, it would likely be positioned at a longer distance than the *N*-oxide oxygen from the hydrogen-bonding partner backbone NH of Asp1222, which results in a weaker activity than the *N*-oxide compounds.

Compound **2** was screened broadly against many other kinases, and some of its kinase activitites are shown in Table 4. In addition to potent Met kinase inhibitory activity, compound **2** also exhibits potent inhibitory activities notably against Flt-3 (IC_{50} = 4 nM) and VEGFR-2 (IC_{50} = 27 nM) kinases with weaker activities against LCK and c-kit kinases.

In Vitro Metabolic Stability and Pharmacokinetics of Compound 2. Compound **2** showed good metabolic stability in both human and mouse liver microsomes with metabolic rates of <0.01 and 0.055 (nmol/min)/mg of protein, respectively, at a concentration of 3 μM. Pharmacokinetic parameters of compound **2** in mice after iv (5 mg/kg) and po (10 mg/kg) dosing are summarized in Table 5. The systemic serum clearance (Cl) of compound **2** was about 10% of hepatic blood flow, and the large steady state volume of distribution (V_{ss} = 1.6 L/kg) is indicative of extensive extravascular distribution. Compound **2** demonstrated a favorable half-life ($t_{1/2}$ = 2.2 h) and mean residence time (MRT = 4.5 h) after po dosing. The measured oral bioavailability of compound **2** was 100% from a solution formulation of 70:30 PEG 400/water. The serum protein binding of compound **2** was high (99.4 ± 0.3% and 99.9 ± 0% in mouse and human serum, respectively) using the equilibrium dialysis method at a concentration of 10 μM.

In Vivo Antitumor Activity. To determine the in vivo antitumor effects due to Met kinase inhibition, compound **2** was

Scheme 4[a]

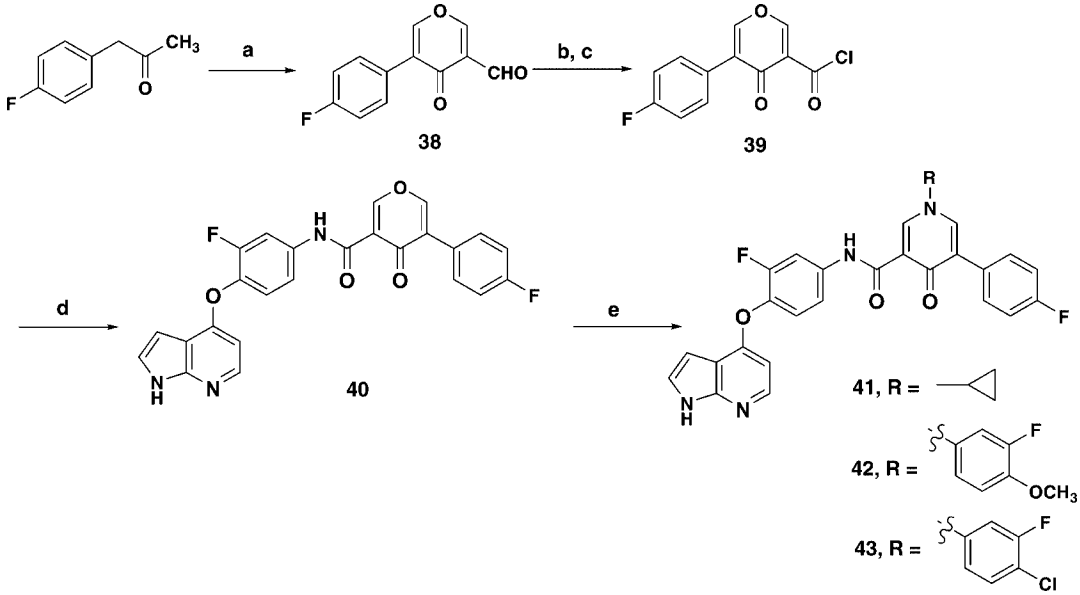

[a] Reagents and conditions: (a) $POCl_3$, DMF, 59%; (b) oxone, THF/H_2O, room temp, 2 h, 78%; (c) $SOCl_2$, CH_2Cl_2, room temp, 1 h, 100%; (d) **8**, 2,6-lutidine, CH_2Cl_2, 0 °C, 1 h, 52%; (e) RNH_2, THF, room temp, 14 h, 43−61%.

Scheme 5[a]

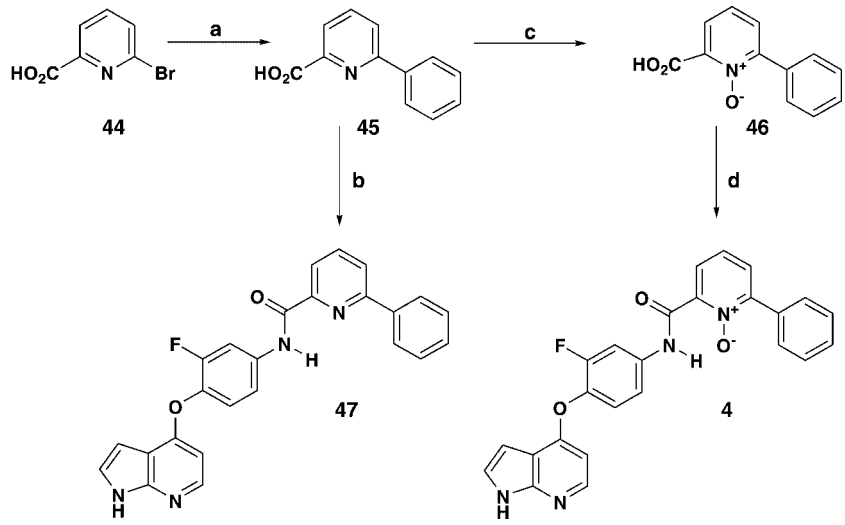

[a] Reagents and conditions: (a) $C_6H_5B(OH)_2$, $PdCl_2[(t\text{-}Bu)_2P(OH)]_2$, Cs_2CO_3, DMF/H_2O, 110 °C, 24 h, 18%; (b) **8**, EDCI, HOBt, DMF, room temp, overnight, 19%; (c) *m*-CPBA, K_2HPO_4, CH_2Cl_2, 60 °C, overnight, 68%; (d) **8**, EDCI, HOBt, DMF, room temp, overnight, 54%.

evaluated against GTL-16 human gastric carcinoma cell line xenografts in nude mice. Good in vivo efficacy was observed at multiple dose levels, as shown in Figure 4. Treatment of compound **2** (po, qd) was initiated 14 days after tumor implantation, at which time tumors were staged to a volume of approximately 125 mm^3. Antitumor activity of **2** was dose proportional. Tumor regressions were observed at 50 and 100 mg/kg, and 100 mg/kg was determined to be the maximum tolerated dose.[23] At 25 mg/kg, this compound induced complete tumor stasis, and the minimum efficacious dose was identified at 12.5 mg/kg, based on greater than or equal to 50% tumor growth inhibition for more than one tumor volume doubling time (7 days). Compound **2**, however, was ineffective at the 6.25 mg/kg dose level. Although we cannot quantify the level of contribution from VEGFR-2 inhibition to the antitumor efficacy of compound **2**, it is likely VEGFR-2 inhibition contributed to the in vivo antitumor activity because of its important role in angiogenesis.[24] In order to confirm the in vivo antitumor activity of compound **2** in the GTL-16 model is due to inhibition of Met kinase phosphorylation levels of the Met protein in the GTL-16, tumor extracts from the tumor bearing animals were examined (Figure 5). Both subefficacious (6.25 mg/kg) and maximally efficacious (25 mg/kg) dose levels were evaluated. As indicated in Figure 5, Met receptor phosphorylation remained relatively unchanged at the subefficacious dose (6.25 mg/kg). At the maximally efficacious dose (25 mg/kg), complete and sustained inhibition of Met receptor phosphorylation was observed up to 8 h, and at 24 h, phosphorylated Met levels began returning to control levels. The Met receptor phosphorylation levels are consistent with the in vivo antitumor efficacy results demonstrated by the compound.

Conclusions

Replacement of the *N*-acylurea moiety in pyrrolopyridine substituted analogue **1** with the conformationally constrained 2-pyridone, 4-pyridone, and pyridine *N*-oxide in analogues **2**−**4**

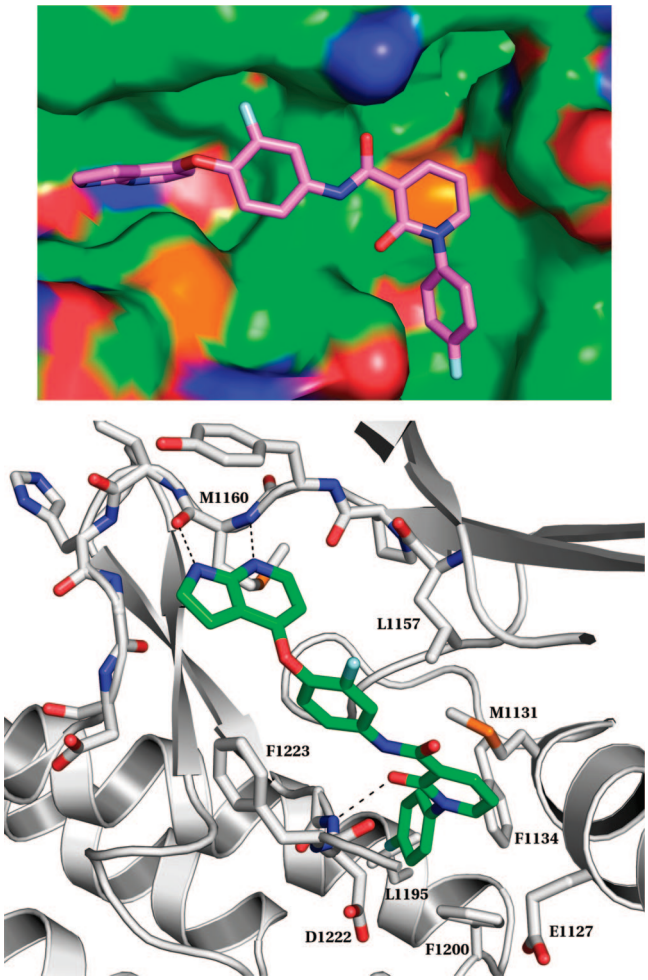

Figure 3. Surface representation and depiction of the binding of compound **2** to the Met kinase domain in X-ray crystal structure.

resulted in a series of potent Met kinase inhibitors. Many of these analogues also demonstrated potent antiproliferative cellular activity in the Met-dependent gastric carcinoma GTL-16 cell line while lacking cellular activity against the Met-independent N87 cell line. Compound **2** also possesses potent inhibitory activity against Flt-3 and VEGFR-2 kinases. Compound **2** showed favorable metabolic and pharmacokinetic properties, and it demonstrated good in vivo efficacy in a GTL-16 human gastric carcinoma xenograft model upon oral administration in nude mice. Tumor regressions were observed in the GTL-16 tumor model at 50 and 100 mg/kg, and the minimum efficacious dose was 12.5 mg/kg. Phosphorylation of the Met receptor in GTL-16 tumor extracts decreased in a time and dose dependent manner, consistent with the in vivo antitumor efficacy of the Met-driven GTL-16 tumor model.

Experimental Section

All new compounds were homogeneous by thin layer chromatography and reversed-phase HPLC (>99%). Flash chromatography was carried out on E. Merck Kieselgel 60 silica gel (230−400 mesh). All the reaction solvents used such as tetrahydrofuran (THF), *N*,*N*-dimethylformamide (DMF), and dichloromethane (CH_2Cl_2) were anhydrous solvents that were purchased from Aldrich Chemical Co. EDCI, HOBT, and TFA refer to ethyl dimethylaminopropylcarbodiimide hydrochloride salt, 1-hydroxybenzotriazole, and trifluoroacetic acid, respectively. Preparative HPLC was run on YMC OD S-10 50 mm × 500 mm column eluting with a mixture of solvents A and B (starting from 10% of solvent B to 100% solvent B over 30 min gradient time; solvent A, 10% MeOH−90% H_2O−0.1% TFA; solvent B, 90% MeOH−10% H_2O−0.1% TFA; flow rate 84 mL/min; UV 220 nm). ^1H and ^{13}C NMR spectra were obtained on a JEOL 500 MHz Eclipse NMR spectrometer operating at 500.16 and 125.77 MHz, respectively. Chemical shifts are

Table 2. SAR of 4-Pyridone Analogues

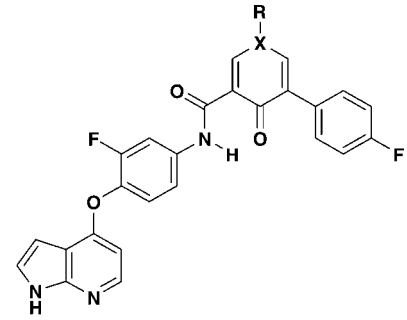

Compd #	R	X	IC$_{50}$ (nM) Met (Biochemical)	GTL-16 (Cellular)	N87
3	H	N	2.8 ± 0.0	70	1240
34	CH_3	N	3.1 ± 0.1	150	2615
37	CH_2CH_2OH	N	3.8 ± 0.1	280	>5000
41	Cyclopropyl	N	3.4 ± 0.1	60	>5000
42	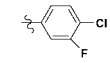	N	5 ± 0.1	200	>5000
43	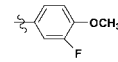	N	2.3 ± 0.0	130	>5000
40	–	O	1400 ± 28.3	>10,000	NT

Table 3. SAR of Pyridine and Pyridine *N*-Oxide Analogues

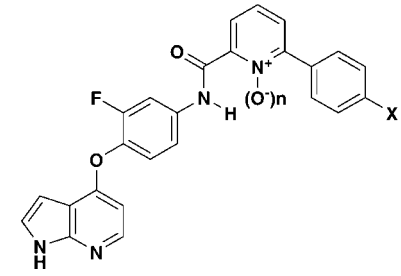

compd	*n*	X	IC$_{50}$ (nM) Met (biochemical)	GTL-16 (cellular)	N87 (cellular)
47	0	H	470 ± 77.8	NT	NT
4	1	H	1.3 ± 0.1	40	>5000
49	1	F	1.8 ± 0.2	40	4900

Table 4. In Vitro Kinase Inhibition of **2**

protein kinase	IC$_{50}$ (nM)
Met	1.9
Flt-3	4
VEGFR-2	4 27
LCK	290
c-kit	610
CDK2/cyclin E	>1000
PKCα	>30000
PKA	>30000
IGF-1R	>5000
InsR	>5000
MK-2	>10000

Table 5. Pharmacokinetic Properties of Compound **2** in Mice[a]

	iv dose	po dose
dose (mg/kg)	5	10
C_{max} (μM)		11.5
T_{max} (h)		0.5
AUC_{0-24h} (μM·h)	19.8	50.2
$T_{1/2}$ (h)	2.5	2.2
MRT (h)	3.0	4.5
clearance ((mL/min)/kg)	9.2	
V_{ss} (L/kg)	1.6	
F (%)		100

[a] Composite serum concentration−time profiles were constructed for the PK analysis. Vehicle: PEG 400/water (70:30).

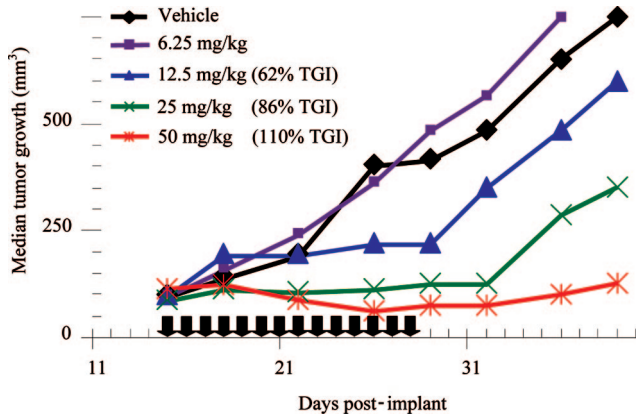

Figure 4. Antitumor activity of compound **2** in the GTL-16 human gastric carcinoma model (% TGI on day 29).

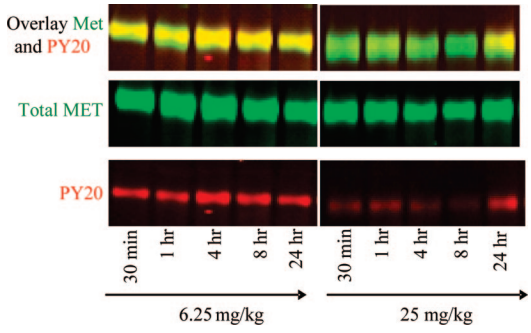

Figure 5. Phospho Met protein levels in GTL-16 tumor extracts. Met and pMet proteins were simultaneously detected in GTL-16 tumor extracts using two IR fluorophores. Proteins were immunoprecipitated using an anti-Met antibody and resolved by SDS−PAGE. Immunoblots were incubated with rabbit anti-Met and mouse anti-PY-20 primary antibodies, followed by Alexa Fluor 680 goat antimouse (red) and IRDye 800 goat antirabbit (green). Both colors were imaged in a single scan.

reported as ppm downfield from an internal tetramethylsilane standard. The abbreviations of br s, d, t, and m in ^{1}H NMR refer to broad singlet, doublet, triplet, and multiplet, respectively. Melting points are uncorrected.

4-(2-Fluoro-4-nitrophenoxy)-1*H*-pyrrolo[2,3-*b*]pyridine (7). A mixture of chloropyrrolopyridine **5** (457 mg, 3.0 mmol), 2-fluoro-4-nitrophenol **6** (703 mg, 4.2 mmol), and *N*,*N*-diisopropylethylamine (583 mg, 4.2 mmol) in 1-methyl-2-pyrrolidinone (NMP) (3 mL) was heated at 200 °C under microwave irradiation for 1 h. The reaction mixture was diluted with EtOAc (150 mL), washed with saturated aqueous KH_2PO_4 solution and Na_2CO_3 (aqueous 1 M), and dried over Na_2SO_4. The product was purified by flash column chromatography (silica gel, eluting with CH_2Cl_2 to 30% EtOAc/CH_2Cl_2) to afford **7** as a brown solid (350 mg, 43%), mp 221−223 °C. HPLC/UV purity 95%; ^{1}H NMR (DMSO-d_6) δ 11.99 (br s, 1H), 8.43 (dd, J = 13.4, 2.7 Hz, 1H), 8.20 (d, J = 5.42 Hz, 1H), 8.15 (dd, J = 13.0, 2.7 Hz, 1H), 7.45 (m, 2H), 6.73 (d, J = 5.33 Hz, 1H), 6.25 (d, J = 5.33 Hz, 1H); ^{13}C NMR (DMSO-d_6) δ 152.4 (d, J_{CF} = 217.2 Hz), 151.3, 148.2, 144.3, 143.7 (d, J_{CF} = 7.7 Hz), 144.3, 126.0, 121.4, 121.3, 113.5 (d, J_{CF} = 23 Hz), 110.3, 103.6, 96.6. HRMS for $C_{13}H_8N_3O_3F$ $(M + H)^+$ calcd 274.0622, found 274.0623.

Table 6. Summary of the Crystallographic Data Collection, Reduction, and Refinement

parameter	**2** bound to Met kinase protein
space group	*P*21 21 21
a (Å)	43.040
b (Å)	49.137
c (Å)	159.324
max observed resolution (Å)	2.40 (2.40−2.49)
no. of observations	41954 (2165)
no. of unique reflections	10949 (897)
R_{symm} (%)	14.4 (46.7)
mean $I/\sigma I$	10. 0 (1.1)
completeness (%)	81.3 (69.9)
refinement program	BUSTER-TNT
R-factor (%)	20.90 (22.42)
R_{free} (%)	27.24 (25.03)
av *B*-factor (protein) (Å^2)	71.58
av *B*-factor (ligand) (Å^2)	49.02
no. of residues in final model	293
no. of atoms	2419
no. of protein atoms	2323
no. of ligand atoms	34
no. of solvent atoms	62
rms (bond) (Å)	0.006
rms (angle) (deg)	0.866
rms (torsion) (deg)	24.454

4-(1*H*-Pyrrolo[2,3-*b*]pyridin-4-yloxy)-3-fluoroaniline (8). To a suspension of nitro compound **7** (300 mg, 1.1 mmol) in THF (5 mL) and MeOH (10 mL) were added zinc powder (350 mg, 5.5 mmol) and ammonium chloride (294 mg, 5.5 mmol). The mixture was stirred at room temperature overnight. The reaction mixture was filtered through a pad of Celite and rinsed with methanol, and the filtrate was concentrated in vacuo. The product was purified by flash column chromatography (silica gel, eluting with 1−5% MeOH in CH_2Cl_2) to afford the **8** (205 mg, 77%) as an off-white solid, mp 185−188 °C. HPLC/UV purity 95%; ^{1}H NMR (DMSO-d_6) δ 11.67 (br s, 1H), 8.02 (m, 1H), 7.32 (m, 1H), 7.01 (t, J = 8.8, 1H), 6.51 (dd, J = 13.2, 2.8 Hz, 1H), 6.43 (dd, J = 8.8, 2.8 Hz, 1H), 6.28 (d, J = 5.0 Hz, 1H), 6.24 (m, 1H), 5.42 (s, 2H); ^{13}C NMR (DMSO-d_6) δ 158.3, 154.7 (d, J_{CF} = 241.6 Hz), 151.0, 148.2 (d, J_{CF} = 10.7 Hz), 144.2, 130.1, 124.4, 124.2, 110.0, 109.3, 101.4 (d, J_{CF} = 23 Hz), 100.1, 96.9; HRMS for $C_{13}H_{10}N_3O_3F$ $(M + H)^+$ calcd 244.0881, found 244.0881.

Methyl 1-(4-Fluorophenyl)-2-oxo-1,2-dihydropyridine-3-carboxylate (11). To a solution of pyran **9** (30.0 g, 195 mmol, Aldrich) in DMF (175 mL) at 0 °C was added 4-fluoroaniline **10** (18.6 mL, 196 mmol), and the reaction mixture was stirred for 7 h. To the reaction mixture was added EDCI·HCl (48.6 g, 254 mmol) and DMAP (6.0 g, 49 mmol) at room temperature, and it was stirred overnight. Most of the solvent was removed in vacuo, and the residue was diluted with water and ethyl acetate. The EtOAc layer was separated, washed with brine, dried over $MgSO_4$, and concentrated in vacuo to obtain a semisolid material. It was triturated with *i*-PrOH to obtain the first crop of **11** (24.1 g). The filtrate solution was concentrated in vacuo to a small volume which was mixed with diethyl ether, and the mixture was stirred for 30 min. The solid was filtered to give light-yellow solid of a second crop of **11** (6.5 g) (total 30.6 g, 64%), mp 101−104 °C. HPLC/UV purity 100%; ^{1}H NMR (DMSO-d_6) δ 8.10 (dd, J = 7.2, 2.2 Hz, 1H), 7.93 (dd, J = 7.2, 2.2 Hz, 1H), 7.46−7.47 (m, 2H), 7.32−7.37 (m, 2H), 6.39 (dd, J = 7.2, 7.2 Hz, 1H) 3.76 (s, 3H); ^{13}C NMR (DMSO-d_6) δ 164.7, 160.3 (d, J_{CF} = 245.9 Hz), 157.8, 144.5, 143.8, 136.4, 128.9 (d, J_{CF} = 7.6 Hz), 120.4, 115.6 (d, J_{CF} = 22.9 Hz), 104.2, 51.5. Anal. ($C_{13}H_{10}NO_3F$) C, H, N, F.

1-(4-Fluorophenyl)-2-oxo-1,2-dihydropyridine-3-carboxylic Acid (12). A mixture of methyl ester **11** (30.0 g, 121 mmol) and 2 N aqueous NaOH (160 mL) in methanol (30 mL) was heated at 65 °C for 1.5 h. To the reaction mixture was added 2 N HCl solution with stirring at room temperature (pH 1.0). The precipitate that formed was filtered, washed with a small amount water, and dried to obtain the desired acid **12** (28.3 g, 99%) as a white solid, mp 213−215 °C. HPLC purity 99%; ^{1}H NMR (DMSO-d_6) δ 14.22 (br s, 1H), 8.47 (dd, J = 7.1, 2.2 Hz, 1H), 8.19 (dd, J = 6.6, 2.2 Hz, 1H), 7.59−7.63 (m, 2H), 7.39−7.44 (m, 2H), 6.78 (dd, J = 6.6, 7.1 Hz, 1H); ^{13}C NMR (DMSO-d_6) δ 164.3, 163.4 (d, J_{CF} = 245.9 Hz), 160.8, 146.0, 144.9, 135.1, 128.8 (d, J_{CF} = 7.6 Hz), 117.1, 115.9 (d, J_{CF} = 22.9 Hz), 108.0. Anal. ($C_{12}H_8NO_3F$) C, H, N, F.

***N*-(4-(1*H*-Pyrrolo[2,3-*b*]pyridin-4-yloxy)-3-fluorophenyl)-1-(4-fluorophenyl)-2-oxo-1,2-dihydropyridine-3-carboxamide (2).** To a heterogeneous mixture of pyrrolopyridine **8** (11.5 g, 47.2 mmol), acid **12** (11.0 g, 47.2 mmol), and 2-(1*H*-benzotriazole-1-yl)-1,1,3-tetramethyluronium tetrafluoroborate (TBTU) (16.7 g, 51.9 mmol) in DMF/CH_3CN (1:1, 200 mL) at 0 °C was added diisopropylethylamine (24.6 mL, 141 mmol) with stirring. Upon addition of diisopropylethylamine, the mixture became homogeneous. The reaction mixture was allowed to warm to room temperature and was stirred for 2 h. Additional TBTU (3.0 g, 9.40 mmol), **12** (1.10 g, 4.72 mmol), and diisopropylethylamine (4.90 mL, 28.3 mmol) were added to the reaction mixture, and stirring was continued for 3 h at room temperature. The reaction mixture was quenched with aqueous 1 N NaOH, and the resultant solution was stirred for 30 min at room temperature. The reaction mixture was concentrated in vacuo, and the resulting slurry was diluted with water. The precipitated solid was filtered, and it was washed with aqueous 10% NaOH followed by water. The solid was dried by azetroping with 3/1 MeOH/toluene. This procedure was repeated 3 times. Purification was accomplished by preabsorbing the crude product on Celite and loading the preabsorbed material on a silica gel flash chromatography column. The product was eluted using a 0−1.5% MeOH in $CHCl_3$ gradient. The appropriate fractions were collected and concentrated in vacuo and dried to obtain **2** (16.6 g, 81% yield) as a white solid, mp 212−214 °C. ^{1}H NMR (DMSO-d_6) δ 12.10 (br s, 1H), 11.78 (br s, 1H), 8.59 (dd, J = 7.3, 2.1 Hz, 1H), 8.14 (d, J = 2.1 Hz, 1H), 8.12 (d, J = 2.1 Hz, 1H), 8.05 (dd, J = 20.5, 5.4 Hz, 1H), 7.62 (m, 2H), 7.42 (m, 5H), 6.73 (t, J = 7.1 Hz, 1H), 6.39 (d, J = 5.5 Hz, 1H), 6.26 (m, 1H); ^{13}C NMR (DMSO-d_6) δ 161.78 (d, J = 246.68 Hz), 161.55, 160.64, 157.05, 154.82, 153.21 (d, J = 244.14 Hz), 151.07, 144.93, 144.20, 144.15,136.24, 129.33, 129.24, 124.86, 123.84, 120.14, 116.41, 116.18, 115.95, 109.36, 108.67, 108.44, 106.99, 100.77, 96.72; MS (ESI) 459 (M + H)$^+$. Anal. ($C_{25}H_{16}N_4O_3F_2$) C, H, N, F. Karl Fischer/water analysis KF water = 0.20 wt %.

***N*-(4-(1*H*-Pyrrolo[2,3-*b*]pyridin-4-yloxy)-3-fluorophenyl)-1-(4-fluorophenyl)-2-oxo-1,2-dihydropyridine-3-carboxamide Hydrochloride Salt (2·HCl).** Compound **2** (40.0 g, 87.3 mmol, 1.0 eq) was suspended in 7:2 THF/MeOH (900 mL), and the heterogeneous solution was cooled to 0 °C. Anhydrous 4 M HCl in dioxane (40.0 mL, 160 mmol, 1.8 equiv) was added in portions, at which point the reaction mixture became homogeneous. After the mixture was stirred for 10 min at 0 °C, a thick white precipitate formed and the reaction mixture continued to be stirred for 1 h at 0 °C. The reaction mixture was concentrated in vacuo, and the resultant solid was triturated with diethyl ether. The solid was filtered, washed with additional diethyl ether, and dried under high vacuum for 12 h. The resultant white solid afforded the product **2** (43 g, 99%) as a mono HCl salt, mp 274−277 °C (dec). HPLC purity 99%; ^{1}H NMR (DMSO-d_6) δ 12.79 (br s, 1H), 12.15 (br s, 1H), 8.59 (dd, J = 7.4, 2.2 Hz, 1H), 8.31 (d, J = 6.3 Hz, 1H), 8.14 (dd, J = 6.6, 1.9 Hz, 1H), 8.08 (dd, J = 12.92, 2.20 Hz, 1H), 7.61 (m, 2H), 7.58 (m, 1H), 7.55 (m, 1H), 7.50 (t, J = 8.8 Hz, 1H), 7.43 (t, J = 8.8 Hz, 2H), 6.74 (m, 1H), 6.73 (d, J = 3.3 Hz, 1H), 6.50 (d, J = 3.0 Hz, 1H); ^{13}C NMR (DMSO-d_6) δ 161.79 (d, J = 246.68 Hz), 161.75, 161.69, 160.59, 153.32 (d, J = 244.14 Hz), 145.00, 144.24, 143.91, 139.06, 137.65 (d, J = 7.63 Hz), 136.17, 135.65 (d, J = 12.72 Hz), 129.26 (2 carbons, d, J = 7.63 Hz), 127.15, 123.95, 120.03, 116.65, 116.06 (2 carbons, d, J = 7.63 Hz), 111.86, 108.64 (d, J = 22.89 Hz), 107.01, 101.45, 98.58; MS (ESI) 459 (M + H)$^+$. Anal. ($C_{25}H_{16}N_4O_3F_2$·1.0HCl) C, H, N, F, Cl. Karl Fischer/water analysis KF water = 0.17 wt %.

***N*-(4-(1*H*-Pyrrolo[2,3-*b*]pyridin-4-yloxy)-3-fluorophenyl)-2-oxo-1-phenyl-1,2-dihydropyridine-3-carboxamide (13).** HPLC purity 97%; ^{1}H NMR (acetone-d_6) δ 13.40 (br s, 1H), 12.32 (br s, 1H), 8.67 (dd, J = 7.1, 2.2 Hz, 1H), 8.43 (d, J = 6.6 Hz, 1H), 8.18 (dd, J = 13.2, 2.2 Hz, 1H), 8.03 (dd, J = 6.6, 2.2 Hz, 1H), 7.72−7.48 (m, 8H), 6.89 (d, J = 6.6 Hz, 1H), 6.75 (t, J = 6.3 Hz, 1H), 6.58 (d, J = 3.3 Hz, 1H); MS (ESI) 441 (M + H)$^+$.

***N*-(4-(1*H*-Pyrrolo[2,3-*b*]pyridin-4-yloxy)-3-fluorophenyl)-1-*tert*-butyl-2-oxo-1,2-dihydropyridine-3-carboxamide (14).** HPLC purity 95%; ^{1}H NMR (CD_3OD) δ 8.54 (dd, J = 7.2, 2.2 Hz, 1H), 8.28 (d, J = 7.1 Hz, 1H), 8.17 (dd, J = 7.1, 1.7 Hz, 1H), 8.07 (dd, J = 12.7, 2.2 Hz, 1H), 7.53 (d, J = 3.8 Hz, 1H), 7.52 (s, 1H), 7.50 (d, J = 1.1 Hz, 1H), 7.44 (t, J = 8.8 Hz, 1H), 6.85 (d, J = 6.6 Hz, 1H), 6.65 (d, J = 3.8 Hz, 1H), 6.55 (t, J = 7.1 Hz, 1H), 1.78 (s, 9H); MS (ESI) 421 (M + H)$^+$.

***N*-(4-(1*H*-Pyrrolo[2,3-*b*]pyridin-4-yloxy)-3-fluorophenyl)-1-cyclopropyl-2-oxo-1,2-dihydropyridine-3-carboxamide (15).** HPLC purity 95%; ^{1}H NMR (DMF-d_7) δ 12.56 (br s, 1H), 12.00 (br s, 1H), 8.55 (dd, J = 7.2, 2.2 Hz, 1H), 8.22 (d, J = 5.5 Hz, 1H), 8.17 (dd, J = 13.2, 2.2 Hz, 1H), 8.13 (dd, J = 6.6, 2.2 Hz, 1H), 7.58−7.50 (m, 3H), 6.65 (t, J = 7.2 Hz, 1H), 6.57 (d, J = 5.5 Hz, 1H), 6.43 (d, J = 2.2 Hz, 1H), 3.60−3.62 (m, 1H), 1.19−1.20 (m, 2H), 1.10−1.11 (m, 2H); MS (ESI) 405 (M + H)$^+$.

***N*-(4-(1*H*-Pyrrolo[2,3-*b*]pyridin-4-yloxy)-3-fluorophenyl)-1-isopentyl-2-oxo-1,2-dihydropyridine-3-carboxamide (16).** Mp 183−184 °C; HPLC purity 98%; ^{1}H NMR ($CDCl_3$) δ 12.26 (br s, 1H), 9.05 (br s, 1H), 8.62 (d, 1H, J = 5.04 Hz), 8.14 (d, 1H, J = 5.56 Hz), 7.95 (d, J = 12.32, 2.52 Hz, 1H), 7.58 (dd, 1H, J = 6.56, 2.28 Hz, 2H), 7.40−7.45 (m, 1H), 7.16−7.24 (m, 2H), 6.51 (t, J = 7.08 Hz, 1H), 6.42−6.47 (m, 2H), 4.09 (t, J = 7.52 Hz, 2H), 1.65−1.80 (m, 3H), 1.02 (d, J = 6.28 Hz, 6H); MS (ESI) 435 (M + H)$^+$.

***N*-(4-(1*H*-Pyrrolo[2,3-*b*]pyridin-4-yloxy)-3-fluorophenyl)-1-(4-fluorobenzyl)-2-oxo-1,2-dihydropyridine-3-carboxamide (17).** Mp 140−142 °C (dec); ^{1}H NMR (DMSO-d_6) δ 12.43 (br s, 1H), 12.27 (br s, 1H), 8.51 (dd, J = 7.2, 1.9 Hz, 1H), 8.36 (dd, J = 6.5 Hz, 2.0 Hz, 1H), 8.26 (d, J = 6.1 Hz, 1H), 8.07 (dd, J = 12.90, 2.1 Hz, 1H), 7.55−7.49 (m, 5H), 7.48−7.24 (m, 2H), 6.71 (t, J = 6.89 Hz, 1H), 6.66−6.64 (m, 1H), 6.43 (br s, 1H), 5.32 (s, 2H); MS (ESI) 473 (M + H)$^+$. Anal. ($C_{26}H_{18}N_4O_3F_2$·1.12HCl·1.44H_2O) C, H, N, Cl.

***N*-(4-(1*H*-Pyrrolo[2,3-*b*]pyridin-4-yloxy)-3-fluorophenyl)-2-oxo-1-(pyridin-2-yl)-1,2-dihydropyridine-3-carboxamide (18).** HPLC purity 97%; ^{1}H NMR (DMF-d_7) δ 12.16 (br s, 1H), 11.99 (br s, 1H), 8.71−8.72 (m, 2H), 8.37 (d, J = 3.9 Hz, 1H), 8.21−7.47 (m, 8H), 6.87 (t, J = 7.2 Hz, 1H), 6.56 (t, J = 5.5 Hz, 1H), 6.42 (d, J = 3.3 Hz, 1H); MS (ESI) 442 (M + H)$^+$.

***N*-(4-(1*H*-Pyrrolo[2,3-*b*]pyridin-4-yloxy)-3-fluorophenyl)-2-oxo-1-(pyridin-3-yl)-1,2-dihydropyridine-3-carboxamide (19).** HPLC purity 97%; ^{1}H NMR (DMF-d_7) δ 12.26 (br s, 1H), 12.18 (br s, 1H), 8.90 (d, J = 2.2 Hz, 1H), 8.78 (d, J = 3.9 Hz, 1H), 8.70 (dd, J = 7.1, 2.2 Hz, 1H), 8.27 (dd, J = 6.6, 2.2 Hz, 2H), 8.17−8.19 (m, 2H), 8.03 (s, 1 H), 7.72−7.50 (m, 3H), 6.86 (t, J = 7.2 Hz, 1H), 6.63 (d, J = 5.5 Hz, 1H), 6.47 (s, 1H); MS (ESI) 442 (M + H)$^+$.

***N*-(4-(1*H*-Pyrrolo[2,3-*b*]pyridin-4-yloxy)-3-fluorophenyl)-1-(4-carbamoylphenyl)-2-oxo-1,2-dihydropyridine-3-carboxamide (20).** Mp 311−313 °C; HPLC purity 96%; ^{1}H NMR (DMF-d_7) δ 12.26 (br s, 1H), 12.21 (br s, 1H), 8.72−8.70 (m, 1H), 8.30−8.15 (m, 6H), 7.75−7.60 (m, 2H), 7.57−7.48 (m, 4H), 6.85−6.83 (m, 1H), 6.63−6.62 (m, 1H), 6.45−6.44 (m, 1H); MS (ESI) 484 (M + H)$^+$.

Ethyl 4-(4-Fluorophenyl)-3-oxobutanoate (24). To a solution of Meldrum's acid **21** (20.0 g, 139 mmol) in anhydrous CH_2Cl_2 (160 mL) was added anhydrous pyridine (28 mL), followed by addition of 4-fluorophenylacetyl chloride **22** (20 mL, 142 mmol) under nitrogen at ice bath temperature. The reaction mixture was

stirred at ice bath temperature for 2.5 h. The reaction mixture was extracted with a mixture of CH_2Cl_2 and aqueous HCl solution (1 N). The organic layer was washed with brine, dried over $MgSO_4$, and concentrated. To the residue was added absolute ethanol (200 mL), and the reaction mixture was heated at 85 °C for 16 h. The solvent was removed in vacuo, and the resulting residue was purified by silica gel chromatography eluting with 0−10% of ethyl acetate in hexane. The desired product **24** was obtained as a colorless oil (15.0 g, 48%). ^{1}H NMR ($CDCl_3$) δ 7.25−7.15 (m, 2H), 7.05−6.98 (m, 2H), 4.18 (q, J = 7.2 Hz, 2H), 3.81 (s, 2H), 3.46 (s, 2H), 1.26 (t, J = 7.2 Hz, 3H); MS (ESI) 225.3 $(M + H)^+$.

Ethyl 5-(4-Fluorophenyl)-4-oxo-1,4-dihydropyridine-3-carboxylate (26). To a solution of **24** (20.1 g, 89.7 mmol) in absolute ethanol (200 mL) was added triazine **25** (7.63 g, 94.2 mmol) followed by addition of 21% NaOEt solution in EtOH (35.2 mL, 94.2 mmol) under nitrogen at room temperature. The resulting mixture was heated at 85 °C for 2 h. The reaction mixture was concentrated to about 20 mL. To the residue was added 1 N aqueous HCl solution with stirring. The precipitate was filtered, washed with distilled water, ethyl acetate, and dried to give **26** as a yellow solid (18.2 g, 78%). ^{1}H NMR ($CDCl_3$) δ 8.97 (s, 1H), 8.55 (s, 1H), 7.58−7.52 (m, 2H), 7.17 (t, J = 8.8 Hz, 2H), 4.50 (q, J = 7.2 Hz, 2H), 1.46 (t, J = 7.2 Hz, 3H); MS (ESI) 262 $(M + H)^+$.

5-(4-Fluorophenyl)-4-oxo-1,4-dihydropyridine-3-carboxylic Acid (27). A mixture of ester **26** (18.2 g, 69.7 mmol) in MeOH (30 mL) and 2 N aqueous NaOH solution (120 mL) was heated for 2 h at 60 °C. After cooling to room temperature, the mixture was poured into 2 N aqueous HCl. The solid that formed was filtered, washed with distilled water and a small amount of ethyl acetate, and dried to give **27** as a light-yellow solid (15.8 g, 97%). ^{1}H NMR (DMSO-d_6) δ 8.60 (s, 1H), 8.24 (s, 1H), 7.72−7.68 (m, 2H), 7.27 (t, J = 8.6 Hz, 2H); MS (ESI) 234.3 $(M + H)^+$. Anal. ($C_{12}H_8FNO_3$) C, H, N, F.

***N*-(4-(1*H*-Pyrrolo[2,3-*b*]pyridin-4-yloxy)-3-fluorophenyl)-5-(4-fluorophenyl)-4-oxo-1,4-dihydropyridine-3-carboxamide (3).** To a suspension of acid **27** (8.0 g, 34.3 mmol) in anhydrous DMF (56 mL) were added HATU (15.65 g, 41.2 mmol) and *i*-Pr_2NEt (18 mL, 104 mmol) at ice bath temperature under nitrogen. The mixture turned into a clear solution after being stirred for 5 min. To the solution was added aniline **8** (7.9 g, 32.5 mmol) slowly. The reaction mixture was stirred for 3 h at room temperature and was poured into aqueous 1 N HCl solution. The solid that formed was filtered, washed with distilled water, and dried. The crude product was purified by silica gel chromatography, eluting with 1−5% of MeOH in CH_2Cl_2 to obtain **3** as a light-yellow solid (5.9 g, 40%), mp 188−190 °C. HPLC purity 97%; ^{1}H NMR (DMF-d_7) δ 13.53 (br s, 1H), 13.03 (br s, 1H), 11.97 (br s, 1H), 9.0 (d, J = 1.2 Hz, 1H), 8.39 (d, J = 1.2 Hz, 1H), 8.37−8.32 (m, 2H), 8.04−7.99 (m, 2H), 7.72−7.61 (m, 3H), 7.49 (m, 2H), 6.67 (d, J = 5.6 Hz, 1H), 6.56 (t, J = 2.4 Hz, 1H); MS (ESI) 459 $(M + H)^+$.

5-Bromo-4-hydroxynicotinic Acid (29). Methyllithium solution in diethyl ether (8.0 mL of 1.5 M solution, 12.0 mmol) was slowly added to a mixture of **28** (3.0 g, 11.9 mmol) in anhydrous THF (25 mL) at −78 °C under argon. After the mixture was stirred for 30 min, *n*-BuLi solution in hexane (15.6 mL of 1.6 M solution, 25.0 mmol) was added to the reaction mixture at −78 °C and it was stirred for 1.5 h at −78 °C. Carbon dioxide gas was bubbled through the mixture for 30 min at −78 °C. To the reaction mixture was added aqueous 4 N HCl solution, and the resulting mixture was concentrated. Water was added to the residue and the solid that formed was filtered, washed with water, and dried to afford **29** as a brown solid (2.2 g, 85%). ^{1}H NMR (DMF-d_7) δ 13.72 (br s, 1H), 8.95 (d, J = 1.1 Hz, 1H), 8.89 (d, J = 1.4 Hz, 1H); MS (ESI) 218 $(M + H)^+$.

Methyl 5-Bromo-1-methyl-4-oxo-1,4-dihydropyridine-3-carboxylate (30). A mixture of acid **29** (2.0 g, 9.17 mmol) and Cs_2CO_3 (18.0 g, 55 mmol) in anhydrous DMF (20 mL) was stirred at room temperature for 20 min under nitrogen. To the mixture was added MeI (3.4 mL, 55 mmol), and the reaction mixture was stirred at room temperature for 4 h. The reaction mixture was concentrated and the residue was purified by silica gel chromatography, eluting with CH_2Cl_2/EtOAc/MeOH (1:1:0.05) to obtain **30** as a yellow solid (1.94 g, 86%). ^{1}H NMR (CD_3OD) δ 8.42 (s, 1H), 8.24 (s, 1H), 3.82 (s, 3H), 3.80 (s, 3H); ^{13}C NMR (CD_3OD) δ 171.0, 165.8, 147.8, 143.9, 119.2, 117.9, 52.3, 44.6; MS (ESI) 246 $(M + H)^+$.

Methyl 5-(4-Fluorophenyl)-1-methyl-4-oxo-1,4-dihydropyridine-3-carboxylate (32). A mixture of **30** (1.80 g, 7.32 mmol), 4-fluorophenylboronic acid **31** (1.43 g, 10 mmol), and K_2CO_3 (1.52 g, 10.2 mmol) in 1,4-dioxane (20 mL) was purged with argon, and $Pd(PPh_3)_4$ (658 mg, 0.57 mmol) was added to the mixture. The reaction mixture was heated for 23 h at 90 °C under argon. The reaction mixture was filtered through a Celite pad and washed with ethyl acetate and the filtrate solution was concentrated and purified by silica gel chromatography, eluting with CH_2Cl_2/EtOAc/MeOH (1:1:0.1) to give **32** as a yellow solid (400 mg, 21%). ^{1}H NMR (CD_3OD) δ 8.40 (d, J = 2.2 Hz, 1H), 7.84 (d, J = 2.2 Hz, 1H), 7.59 (dd, J = 5.5 Hz, 2H), 7.11 (t, J = 8.8 Hz, 2H), 3.81 (s, 6H); MS (ESI) 262 $(M + H)^+$.

5-(4-Fluorophenyl)-1-methyl-4-oxo-1,4-dihydropyridine-3-carboxylic Acid (33). A mixture of **32** (110 mg, 0.42 mmol) in MeOH (5.0 mL) and 2 N aqueous NaOH (1.0 mL) solution was heated at 60 °C for 2 h. After cooling to room temperature, the mixture was poured onto 1 N aqueous HCl solution. The resulting solid was filtered, washed with water, and dried to give **33** as a white solid (90 mg, 86%). ^{1}H NMR (CD_3OD) δ 8.70 (d, J = 2.0 Hz, 1H), 8.18 (d, J = 2.0 Hz, 1H), 7.73−7.70 (m, 2H), 7.23−7.19 (m, 2H), 4.01 (s, 3H); MS (ESI) 248 $(M + H)^+$.

***N*-(4-(1*H*-Pyrrolo[2,3-*b*]pyridin-4-yloxy)-3-fluorophenyl)-5-(4-fluorophenyl)-1-methyl-4-oxo-1,4-dihydropyridine-3-carboxamide (34).** To a mixture of **33** (87 mg, 0.35 mmol) in anhydrous DMF (2.0 mL) were added HATU (174 mg, 0.358 mmol) and *i*-Pr_2NEt (1.0 mL) followed by **8** (92 mg, 0.38 mmol) under nitrogen. The reaction mixture was stirred at room temperature for 1.5 h. The reaction mixture was purified by preparative HPLC to give **34** as a white solid (88 mg, 66%), mp 196−198 °C. HPLC purity 97%; ^{1}H NMR (DMSO-d_6) δ 13.23 (br s, 1H), 12.09 (br s, 1H), 8.69 (d, J = 2.2 Hz, 1H), 8.17−8.16 (m, 2H), 8.03 (dd, J = 2.2, 13.2 Hz, 1H), 7.71 (dd, J = 5.5, 8.2 Hz, 2H), 7.50−7.38 (m, 3H), 7.28 (t, J = 8.8 Hz, 2H), 6.53−6.51 (m, 1H), 6.35 (br s, 1H), 3.92 (s, 3H); HRMS (ESI) calcd for $C_{26}H_{18}F_2N_4O_3$ $(M + H)^+$ 473.1420, found 473.1419.

Methyl 5-Bromo-1-(2-hydroxyethyl)-4-oxo-1,4-dihydropyridine-3-carboxylate (35). (A) To a mixture of acid **29** in anhydrous MeOH (60 mL) at 0 °C was slowly added thionyl chloride (5.0 mL) under nitrogen. The resulting mixture was stirred at 0 °C for 15 min. It was warmed to room temperature and heated at 70 °C for 4 h. The solvent was removed in vacuo, and the residue was triturated with saturated $NaHCO_3$. The solid was filtered and dried to give a light-brown solid of methyl 5-bromo-4-oxo-1,4-dihydropyridine-3-carboxylate (4.93 g, 93%): ^{1}H NMR (DMSO-d_6) δ 12.20 (br s, 1H), 8.26 (s, 2H), 3.73 (s, 3H); MS (ESI) 232.2 $(M + H)^+$.

(B) A mixture of 5-bromo-4-oxo-1,4-dihydropyridine-3-carboxylate (4.0 g, 17.2 mmol) and K_2CO_3 (5.0 g, 34 mmol) in anhydrous DMF (30 mL) was stirred for 30 min at room temperature. To the mixture 2-bromoethnol (3.1 mL, 43 mmol) was added, and the reaction mixture was heated at 50 °C for 22 h under nitrogen. After cooling to room temperature, the reaction mixture was filtered through a Celite pad and washed with ethyl acetate and the filtrate solution was concentrated. The residue was triturated with ether to obtain **35** as a light-yellow solid (4.16 g, 87%). ^{1}H NMR (CD_3OD) δ 8.45 (s, 1H), 8.27 (s, 1H), 4.07 (s, 2H), 3.79 (s, 5H); MS (ESI) 276.18, 278.1 $(M + H)^+$.

5-(4-Fluorophenyl)-1-(2-hydroxyethyl)-4-oxo-1, 4-dihydropyridine-3-carboxylic Acid (36). (A) A mixture of **35** (0.56 g, 2.41 mmol), 4-fluorophenylboronic acid **31** (0.51 g, 3.62 mmol), and K_2CO_3 (0.53 g, 3.61 mmol) in 1,4-dioxane (8.0 mL) was purged with argon. Then $Pd(PPh_3)_4$ (195 mg, 0.17 mmol) was added to the reaction mixture. The reaction mixture was heated at 90 °C for 20 h under argon. The reaction mixture was filtered through a Celite pad and washed with ethyl acetate. The filtrate solution was concentrated and purified by silica gel chromatography, eluting with CH_2Cl_2/EtOAc/MeOH (5:2:0.4) to give the ester of **36** (160 mg,

22%) as a light-yellow solid. ^{1}H NMR (CD_3OD) δ 8.45 (d, J = 2.2 Hz, 1H), 7.90 (d, J = 2.2 Hz, 1H), 7.62−7.58 (m, 2H), 7.12 (t, J = 8.8 Hz, 2H), 4.12 (t, J = 5.0 Hz, 2H), 3.86 (t, J = 5.0 Hz, 2H), 3.83 (s, 3H); MS (ESI) 292 $(M + H)^+$.

(B) A solution of methyl 5-(4-fluorophenyl)-1-(2-hydroxyethyl)-4-oxo-1,4-dihydropyridine-3-carboxylate (160 mg, 0.55 mmol) in MeOH (3 mL) and 6 N aqueous NaOH (0.5 mL) was stirred for 2 h at room temperature. The reaction mixture was acidified with 1 N aqueous HCl solution and the product was extracted with ethyl acetate. The organic layer was washed with brine, dried over $MgSO_4$, and concentrated to give **36** as a light-yellow solid (135 mg, 89%), which was used directly in the next step without further purification. MS (ESI) 278 $(M + H)^+$.

***N*-(4-(1*H*-Pyrrolo[2,3-*b*]pyridin-4-yloxy)-3-fluorophenyl)-5-(4-fluorophenyl)-1-(2-hydroxyethyl)-4-oxo-1,4-dihydropyridine-3-carboxamide (37).** To a mixture of **36** (125 mg, 0.45 mmol) in anhydrous DMF (1.5 mL) were added HATU (206 mg, 0.54 mmol) and *i*-Pr_2NEt (0.5 mL) followed by aniline **8** (115 mg, 0.0.47 mmol) under nitrogen. The reaction mixture was stirred for 1.5 h at room temperature and purified by preparative HPLC to give **37** as a white solid (105 mg, 67%), mp180−182 °C. HPLC purity 96%; ^{1}H NMR (CD_3OD) δ 8.76 (d, J = 2.2 Hz, 1H), 8.31 (d, J = 6.6 Hz, 1H), 8.08−8.06 (m, 2H), 7.67−7.65 (m, 2H), 7.57 (d, J = 3.3 Hz, 1H), 7.51−7.43 (m, 2H), 7.19 (t, J = 8.8 Hz, 2H), 6.91 (d, J = 6.6 Hz, 1H), 6.69 (d, J = 3.3 Hz, 1H), 4.25 (t, J = 5.0 Hz, 2H), 3.93 (t, J = 5.5 Hz, 2H); HRMS (ESI) calcd for $C_{27}H_{20}F_2N_4O_4$ $(M + H)^+$ 503.1526, found 503.1524.

***N*-(4-(1*H*-Pyrrolo[2,3-*b*]pyridin-4-yloxy)-3-fluorophenyl)-5-(4-fluorophenyl)-4-oxo-4*H*-pyran-3-carboxamide (40). (A)** To a solution of aldehyde **38** (218 mg, 1.0 mmol) in THF (5 mL) and water (1 mL) was added oxone (1.84 g, 3 mmol). The reaction mixture was stirred for 2 h at room temperature and concentrated in vacuo. The residue was triturated with water/ether, and the solid that formed was collected by filtration and dried to give 5-(4-fluorophenyl)-4-oxo-4*H*-pyran-3-carboxylic acid as a white solid (183 mg, 78%), mp 175−177 °C. HPLC purity 97%; ^{1}H NMR (DMSO-d_6) δ 13.60 (br s, 1H), 9.04 (s, 1H), 8.67 (s, 1H), 7.68−7.60 (m, 2H), 7.30 (t, J = 8.8 Hz, 2H); MS (ESI) 235 $(M + H)^+$.

(B) To a solution of 5-(4-fluorophenyl)-4-oxo-4*H*-pyran-3-carboxylic acid (200 mg, 0.85 mmol) in CH_2Cl_2 (10 mL) at 0 °C was added thionyl chloride (202 mg, 1.7 mmol). The reaction mixture was stirred for 1 h at room temperature and concentrated in vacuo. The residue was dissolved in a mixed solvent of DMF (2 mL) and CH_2Cl_2 (4 mL) at 0 °C. A solution of **8** (207 mg, 0.85 mmol) in CH_2Cl_2 (1 mL) was added dropwise to the acyl chloride solution followed by the addition of 2,6-lutidine (0.20 mL, 1.70 mmol). The reaction mixture was stirred for 1 h at 0 °C and concentrated in vacuo. Upon addition of cold water (5 mL), solid was precipitated, which was collected and dried to obtain **40** (202 mg, 52%) as a white solid. HPLC purity 98%; ^{1}H NMR (CD_3OD) δ 8.83 (d, J = 2.2 Hz, 1H), 8.34 (d, J = 2.2 Hz, 1H), 8.15 (d, J = 6.0 Hz, 1H), 7.83 (dd, J = 11.0, 2.8 Hz, 1H), 7.70−7.66 (m, 2H), 7.60 (d, J = 10.5 Hz, 1H), 7.55 (t, J = 8.2 Hz, 1H), 7.39 (d, J = 3.3 Hz, 1H), 7.17 (t, J = 8.8 Hz, 2H), 6.70 (d, J = 6.0 Hz, 1H), 6.51 (d, J = 3.3 Hz, 1H); MS (ESI) 460 $(M + H)^+$.

***N*-(4-(1*H*-Pyrrolo[2,3-*b*]pyridin-4-yloxy)-3-fluorophenyl)-1-cyclopropyl-5-(4-fluorophenyl)-4-oxo-1,4-dihydropyridine-3-carboxamide (41).** To a solution of **40** (46 mg, 0.1 mmol) in THF (2.0 mL) at room temperature was added cyclopropanamine (29 mg, 0.5 mmol). The reaction mixture was stirred for 14 h, and concentrated in vacuo. The residue was purified by preparative HPLC to obtain **41** as a white solid (30 mg, 61%), mp 212−214 °C (dec). HPLC purity 98%; ^{1}H NMR (CD_3OD) δ 8.65 (d, J = 2.2 Hz, 1H), 8.16 (d, J = 6.6 Hz, 1H), 7.98 (d, J = 2.8 Hz, 1H), 7.95 (dd, J = 11.0, 2.8 Hz, 1H), 7.57−7.53 (m, 2H), 7.42 (d, J = 3.3 Hz, 1H), 7.36 (d, J = 8.8 Hz, 1H), 7.31 (t, J = 8.3 Hz, 1H), 7.09 (t, J = 8.8 Hz, 2H), 6.70 (d, J = 6.6 Hz, 1H), 6.52 (d, J = 3.8 Hz, 1H), 3.75−3.70 (m, 1H), 1.12−1.08 (m, 4H); MS (ESI) 499 $(M + H)^+$.

***N*-(4-(1*H*-Pyrrolo[2,3-*b*]pyridin-4-yloxy)-3-fluorophenyl)-1-(3-fluoro-4-methoxyphenyl)-5-(4-fluorophenyl)-4-oxo-1,4-dihydropyridine-3-carboxamide (42).** Mp 238−240 °C (dec); HPLC purity 98%; ^{1}H NMR (CD_3OD) δ 8.75 (d, J = 2.2 Hz, 1H), 8.12 (s, 2H), 7.97 (d, J = 12.1 Hz, 1H), 7.64−7.61 (m, 2H), 7.51 (dd, J = 2.7, 11.0 Hz, 1H), 7.42−7.38 (m, 3H), 7.32 (t, J = 8.8 Hz, 1H), 7.23 (t, J = 8.8 Hz, 1H), 7.10 (t, J = 8.8 Hz, 2H), 6.66 (d, J = 6.0 Hz, 1H), 6.51 (d, J = 3.3 Hz, 1H), 3.88 (s, 3H); MS (ESI) 583 $(M + H)^+$.

***N*-(4-(1*H*-Pyrrolo[2,3-*b*]pyridin-4-yloxy)-3-fluorophenyl)-1-(4-chloro-3-fluorophenyl)-5-(4-fluorophenyl)-4-oxo-1,4-dihydropyridine-3-carboxamide (43).** HPLC purity 98%; ^{1}H NMR (CD_3OD) δ 8.82 (d, J = 2.2 Hz, 1H), 8.19 (s, 1H), 8.14 (d, J = 6.6 Hz, 1H), 7.98 (d, J = 12.6 Hz, 1H), 7.71 (dd, J = 2.2, 9.3 Hz, 1H), 7.67 (t, J = 8.3 Hz, 1H), 7.64−7.61 (m, 2H), 7.48 (d, J = 8.3 Hz, 1H), 7.42−7.38 (m, 2H), 7.33 (t, J = 8.2 Hz, 1H), 7.11 (t, J = 8.8 Hz, 2H), 6.67 (d, J = 6.6 Hz, 1H), 6.51 (d, J = 3.8 Hz, 1H); MS (ESI) 587 $(M + H)^+$.

6-Phenylpicolinic Acid (45). A mixture of 6-bromopicolinic acid **44** (2.02 g, 10 mmol), phenylboronic acid (1.22 g, 10 mmol), cesium carbonate (5.0 g, 15 mmol), and $PdCl_2$ [$(t$-Bu$)_2$P(OH)]$_2$ (180 mg, 0.36 mmol, CombiPhos Catalyst, Inc.) in DMF (20 mL) and water (3 mL) was purged with Ar gas and heated at 110 °C for 24 h. The reaction did not proceed any further despite remaining starting materials. The mixture was acidified to pH 6 using 1 N aqueous HCl, and the mixture was extracted with EtOAc (150 mL). The EtOAc layer was dried over Na_2SO_4 and concentrated in vacuo, and the residue was purified by preparative HPLC to obtain **45** as a white solid (350 mg, 18%). HPLC purity 96%; ^{1}H NMR ($CDCl_3$) δ 10.46 (br s, 1H), 8.10 (d, J = 7.7 Hz, 1H), 8.03 (m, 4H), 7.53 (m, 3H); MS (ESI) 200 $(M + H)^+$.

2-Carboxy-6-phenylpyridine 1-Oxide (46). To a solution of phenypicolinic acid **45** (150 mg, 0.75 mmol) in dichloroethane (8 mL) at room temperature was added a solid of *m*-CPBA (300 mg, ∼77% purity, Aldrich), and the mixture was heated at 60 °C overnight. Solid K_2HPO_4 (600 mg) was added to the reaction mixture, and the suspension was heated at 60 °C for 90 min. With addition of more *m*-CPBA (600 mg), the mixture continued to be heated at 60 °C for 30 min. The mixture was directly purified by preparative HPLC to obtain **46** as a white solid (110 mg, 68%). HPLC purity 99%; ^{1}H NMR (DMF-d_7) δ 8.58 (s, 1H), 8.42 (dd, J = 7.7, 2.2 Hz, 1H), 8.10−7.88 (m, 4H), 7.60−7.58 (m, 3H); MS (ESI) 216 $(M + H)^+$.

***N*-(4-(1*H*-Pyrrolo[2,3-*b*]pyridin-4-yloxy)-3-fluorophenyl)-6-phenylpicolinamide (47).** To a solution of acid **45** (48 mg, 0.24 mmol) in DMF (5 mL) at room temperature were added EDCI·HCl (75 mg, 0.39 mmol) and HOBt·hydrate (25 mg, 0.16 mmol) followed by pyrrolopyridine **8** (65 mg, 0.27 mmol). The reaction mixture was stirred at room temperature over the weekend, and the mixture was purified directly by preparative HPLC to obtain **47** as a light-brown solid (25 mg, 19%). HPLC purity 97%; ^{1}H NMR (DMF-d_7) δ 11.93 (br s, 1H), 11.01 (s, 1H), 8.37−8.17 (m, 7H), 7.51−7.57 (m, 6H), 6.52 (d, J = 5.5 Hz, 1H), 6.41(d, J = 3.3 Hz, 1H); MS (ESI) 441 $(M + H)^+$.

2-(4-(1*H*-Pyrrolo[2,3-*b*]pyridin-4-yloxy)-3-fluorophenylcarbamoyl)-6-phenylpyridine 1-Oxide (4). To a solution of *N*-oxide **46** (25 mg, 0.12 mmol) in DMF (3.5 mL) at room temperature were added EDCI·HCl (42 mg, 0.22 mmol) and HOBt·H_2O (18 mg, 0.12 mmol) followed by pyrrolopyridine **8** (40 mg, 0.16 mmol). The reaction mixture was stirred at room temperature overnight, and the mixture was purified directly by preparative HPLC to obtain **4** as a light-brown solid (36 mg, 54%). HPLC purity 96%; ^{1}H NMR (DMF-d_7): δ 14.12 (br s, 1H), 12.10 (br s, 1H), 8.48 (dd, J = 7.7, 2.2 Hz, 1H), 8.24 (d, J = 5.5 Hz, 1H), 8.18 (dd, J = 12.5, 2.2 Hz, 1H), 7.94−7.51 (m, 10H), 6.61 (d, J = 5.5 Hz, 1H), 6.44 (d, J = 3.3 Hz, 1H); MS (ESI) 425 $(M + H)^+$.

2-(4-(1*H*-Pyrrolo[2,3-*b*]pyridin-4-yloxy)-3-fluorophenylcarbamoyl)-6-(4-fluorophenyl)pyridine 1-Oxide (49). (A) 6-(4-Fluorophenyl)picolinic Acid. A solution of 6-bromopicolinic acid (2.02 g, 10 mmol) in DME containing 4 mL of 10% aqueous Na_2CO_3 was purged with Ar gas. To this mixture was added

$Pd(PPh_3)_4$ followed by 2-(4-fluorophenyl)-5,5-dimethyl-1,3,2-dioxaborinane (2.40 g, 11.5 mmol) and EtOH (20 mL). This mixture was purged with Ar gas. The reaction mixture was heated at 100 °C for 2.5 h in a sealed tube. Additional 2-bromopicolinic acid (900 mg) and $Pd(OAc)_2$ were added to the mixture, and it was heated at 100 °C for 4.5 h. Trifluoroactic acid (20 mL) was added to the reaction mixture and concentrated in vacuo, and MeOH (150 mL) was added to the residue. The insoluble material was filtered, the filtrate solution was concentrated, and the residue was purified by flash column chromatography using silica gel and eluting with 9:1 EtOAc/MeOH to 1:2.1:0.3 EtOAc/MeOH/HOAc to provide the desired product (1.0 g, 40% based on borinane starting material) as a white solid. ^{1}H NMR (CD_3OD) δ 8.01 (d, J = 7.7 Hz, 1H), 7.94−7.87 (m, 3H), 7.73 (d, J = 7.7 Hz, 1H), 7.13 (t, J = 8.8 Hz, 2H); MS (ESI) 234 $(M + H)^+$.

(B) 6-(4-Fluorophenyl)picolinic Acid *N*-Oxide. A mixture of picolinic acid derivative (1.0 g, 4.6 mmol), Na_2HPO_4 (1.2 g), and *m*-CPBA (1.1 g, ∼70%) in CH_2ClCH_2Cl (30 mL) was stirred at room temperature for 2 h. Additional Na_2HPO_4 (0.8 g) and *m*-CPBA (1.0 g, ∼70% from Aldrich) was added to the reaction mixture, and it was stirred for 3 h at room temperature. More Na_2HPO_4 (0.5 g) and *m*-CPBA (0.5 g, ∼70%) were added to the reaction mixture, and the mixture was stirred at room temperature overnight. The next morning, $CHCl_3$ (160 mL) and 2 N aqueous HCl (50 mL) were added to the reaction mixture. The organic layer was separated, dried over $MgSO_4$, and concentrated. The residue was purified by flash column chromatography using silica gel and eluting with 7:2.4:0.6 EtOAc/MeOH/HOAc to provide the desired product that was contaminated by a small amount of *m*-CPBA. This impure material was purified by preparative HPLC to obtain the desired *N*-oxide product (175 mg, 16%) as a white solid. ^{1}H NMR (DMF-d_7) δ 8.45 (dd, J = 8.3, 2.2 Hz, 1H), 8.15 (d, J = 2.2 Hz, 1H), 8.13−8.00 (m, 4H), 7.45 (t, J = 8.7 Hz, 2H).

(C) 2-(4-(1*H*-Pyrrolo[2,3-*b*]pyridin-4-yloxy)-3-fluorophenylcarbamoyl)-6-(4-fluorophenyl)pyridine 1-Oxide (49). To a solution of the *N*-oxide obtained above (23 mg, 0.1 mmol) and HOBt (10 mg) in DMF (2 mL) at room temperature was added EDCI·HCl (30 mg, 0.16 mmol) followed by 4-(4-amino-2-fluorophenoxy)pyridine-2-amine (22 mg, 0.1 mmol). The reaction mixture was stirred at room temperature overnight. Direct purification of the reaction mixture by preparative HPLC afforded **49** as a white solid (25 mg, 46%). HPLC purity 98%; ^{1}H NMR (DMF-d_7) δ 14.00 (br s, 1H), 12.14 (br s, 1H), 8.43 (dd, J = 8.0, 2.2 Hz, 1H), 8.15 (dd, J = 12.8, 2.4 Hz, 1H), 8.08 (d, J = 7.1 Hz, 1H), 7.99−7.37 (m, 9H), 6.72 (dd, J = 7.0, 2.4 Hz, 1H), 6.32 (d, J = 2.3 Hz, 1H), 3.7 (br s, 1H); MS (ESI) 417 $(M + H)^+$.

Met Kinase Assay. The kinase reaction consisted of baculovirus expressed GST-Met, 3 μg of poly(Glu/Tyr) (Sigma), 0.12 μCi ^{33}P γ-ATP, 1 μM ATP in 30 μL of kinase buffer (20 mM Tris-Cl, 5 mM $MnCl_2$, 0.1 mg/mL BSA, 0.5 mM DTT). Reactions were incubated for 1 h at 30 °C and stopped by the addition of cold trichloroacetic acid (TCA) to a final concentration of 8%. TCA precipitates were collected onto GF/C unifilter plates (Packard Instrument Co., Meriden, CT) using a Filtermate universal harvester (Packard Instrument Co., Meriden, CT), and the filters were quantitated using a TopCount 96-well liquid scintillation counter (Packard Instrument Co., Meriden, CT). Dose response curves were generated to determine the concentration required to inhibit 50% of substrate phosphorylation (IC_{50}). Compounds were dissolved at 10 mM in dimethylsulfoxide (DMSO) and evaluated at 10 concentrations, in duplicate.

Cellular Proliferation Assay. Inhibition of cell proliferation was assessed by a MTS assay using a CellTiter 96 aqueous nonradioactive proliferation assay kit (Promega). Cells were inoculated into 96-well microtiter plates containing 0.5% fetal calf serum and incubated at 37 °C, 5% CO_2, 95% air, and 100% relative humidity for 24 h prior to addition of drug. At the time of drug addition, one plate of the cell line was processed using the above kit to represent a measurement of the cell population at the time of drug addition. Following drug addition, the plates were incubated for an additional 72 h before processing to measure the cell population. Each compound was tested at eight different concentrations in triplicate, as was a control sample. Growth inhibition of 50% (IC_{50}) is calculated by analysis of the data in Excel using a four-parameter logistic equation with data fitted using the Levenburg−Marquardt algorithm.

Metabolic Stability. The compound was incubated with human liver microsomes purchased from In Vitro Technologies (Baltimore, MD) and pooled from 10 individual donors. The rates of oxidative metabolism were measured under the following conditions: compound (substrate) at 3 μM final concentration; final microsomal protein concentration of approximately 1 mg/mL; 1 mM NADPH; 56 mM of pH 7.4 potassium phosphate buffer. Incubations were performed at 37 °C and were initiated by the addition of the substrate. Incubations were quenched by the addition of one volume of acetonitrile after 10 min. Samples were then analyzed for the parent compound by LC/MS. The rate of metabolism was calculated by determining the nanomoles of parent compound oxidized and dividing it by the time of incubation and the milligrams of protein.

Pharmacokinetic Parameters Obtained in Mice. To evaluate the oral bioavailability of compound **2** in male Balb/C mice, a single dose was administered as a solution in PEG 400/water (70:30) by either tail vein injection (iv, 5 mg/kg) or by oral gavage (po, 10 mg/kg). The mice were fasted overnight prior to dosing and fed 4 h postdose. A total of 18 mice were used in the study (n = 9 each for iv and po group). Three serum samples were collected from each mouse, the first two samples by retro-orbital bleed (∼100 μL/20−25 g mouse) and the third sample by cardiac puncture. Blood samples were collected at 0.17, 0.5, 1, 3, 6, 8, 10, 12, and 24 h time points following iv dosing and at 0.25, 0.5, 1, 3, 6, 8, 10, 12, and 24 h following oral dosing. Blood samples were allowed to clot on ice and were centrifuged, and serum was harvested. Serum samples were stored at −20 °C until analysis. Concentrations of parent compound were later determined by LC/MS/MS. Composite serum concentration−time profiles were constructed for pharmacokinetic analysis.

Serum Protein Binding of Compound 2. The extent of protein binding of compound **2** was determined in mouse and human sera using the equilibrium dialysis method. All experiments were carried out using pooled serum (n = 10 for mice, n = 3 for human) obtained from Bioreclamation Inc. (Hicksville, NY). Compound **2** (1 mM) in acetonitrile was added to serum at a ratio of 1:100 to give a final concentration of 10 μM. Serum samples were dialyzed against 134 mM phosphate buffer (pH 7.4). The Micro-Equilibrium Dialyzer (500 μL chamber volume, Amika Corp., Holliston, MA) containing spiked serum was incubated in a shaking water bath maintained at 37 °C for 4 h. A 10 000 molecular weight cutoff dialysis membrane (Amika Corp., Holliston, MA) was used. All experiments were carried out in triplicate. Aliquots of buffer and serum were taken at 4 h and analyzed by LC/MS/MS. Compound **2** was stable under these conditions over the 4 h incubation period in mouse and human serum. From each dialysis cell, the free and bound drug percentages were calculated as follows: % free = 100 × (concentration in buffer)/(concentration in serum); % bound = 100 − (% free).

In Vivo Antitumor Activity in the Subcutaneously Implanted GTL-16 Xenograft Model in Nude Mice. Female Balb/C athymic (nu+/nu+) mice, 6−8 weeks old, were obtained from Sprague−Dawley Co. (Indianapolis, IN). Animals were provided with food and water ad libitum and housed five per cage. Mice were maintained in accordance with Bristol-Myers Squibb's Institutional Animal Care and Use Committee in accordance with the American Association for Accreditation of Laboratory Animal Care (AAALAC) guidelines for the humane treatment and care of laboratory mice.

GTL-16 tumor fragments maintained by serial passage in vivo were implanted subcutaneously in the hind flank using an 18 g trocar. Approximately 2 weeks after implant, when tumor sizes reached 100−150 mm^3, oral dosing was initiated using gavage needles with either compound at the indicated concentrations or vehicle (7:3 PEG 400/H_2O) in the control group. Tumor growth was assessed twice weekly by vernier caliper measurement. Group sizes were n = 8 or 9.

Antitumor activity was determined by calculating the maximum percent tumor growth inhibition (TGI) of treated animals using the formula % TGI = $\{(C_t - T_t)/(C_t - C_0)\} \times 100$, where C_t is the median tumor volume (mm^3) of vehicle treated control (C) mice at time t. T_t is the median tumor volume of treated mice (T) at time t. C_0 is the median tumor volume of control mice at time 0. Activity is defined as a continuous % TGI > 50% for at least one tumor volume doubling time after the start of drug treatment.

Measurement of Phospho Met Protein Levels in GTL-16 Tumor Extracts. GTL-16 human gastric carcinoma cell line xenografts were implanted in nude mice and allowed to grow to 200−300 mm^3 as previously described. Mice were given a single oral dose of compound **2**. At the indicated time points, mice were sacrificed and tumors immediately excised and snap-frozen in liquid nitrogen. Tumors were homogenized and lysed in ice cold buffer containing 20 mM Tris, 0.12 M NaCl, 0.2 mM EDTA, 1% Triton, 5% glycerol, 1 mM sodium vanadate, and 40 μM ammonium molybdate, with protease inhibitors (Complete Tabs, Boehringer Mannheim). The protein concentration of tumor lysates was determined using a BCA protein assay (Pierce). Approximately 500 μg of total protein was immunoprecipitated using anti-hMet clone C-12 antibody (Santa Cruz Biotechnology) linked to immunopure immobilized protein A/G resin (Pierce) for 3 h in lysis buffer, shaking at 4 °C. Lysates were washed 3 times and resuspended in Lane Marker Reducing Sample Buffer (Pierce). Protein was denatured and separated on a 7.5% polyacrylamide gel (BioRad) and transferred onto pretreated nitrocellulose membrane (BioRad). Membranes were blocked using LiCor Odyssey blocking buffer. Antibodies were diluted in blocking solution containing 0.1% Tween-20. Two color Western blots were performed using rabbit anti-hMet C-12 antibody (Santa Cruz Biotechnology) and mouse anti-phosphotyrosine PY-20 antibodies (BD Transduction Laboratories). For detection, goat antimouse Alexa Fluor 680 (Molecular Probes) and goat antirabbit IRDye 800 (Rockland Immunochemicals) antibodies diluted 1:10000 were utilized. Blots were incubated with primary antibodies simultaneously for 2 h at room temperature, washed with Tris-buffered saline, and incubated with both IR-labeled secondary antibodies for 1 h at room temperature. Blots were imaged and quantified using the Li-Cor Odyssey imaging system.

Crystal Structure of Met Kinase Complexed with Compound 2. Crystals of the Met kinase domain (1067−1378) complexed with compound **2** were grown at room temperature by the hanging drop vapor diffusion method. The hanging drop consisted of 10λ of the concentrated Met kinase complex mixed with an equal volume of reservoir solution containing 12% MEPEG 5k, 0.1 M Hepes (pH 7.1), and 11% 2-propanol. Crystals were flash-frozen in cryoprotectant containing 15% glycerol, and data were collected at the IMCA-CAT beamline ID17 at the Advanced Photon Source, Argonne National Laboratory, Argonne, IL (Table 6).

Note Added after ASAP Publication. This manuscript was released ASAP on August 9, 2008 with an error in Scheme 1. The correct version was released on August 19, 2008.

Supporting Information Available: HPLC and elemental analysis data for key compounds. This material is available free of charge via the Internet at http://pubs.acs.org.

References

(1) Ma, P. C.; Maulik, G.; Christensen, J.; Salgia, R. c-Met: structure, functions and potential for therapeutic inhibition. *Cancer Metastasis Rev.* **2003**, *22*, 309–325.

(2) Trusolino, L.; Comoglio, P. M. Scatter-factor and semaphorin receptors: cell signaling for invasive growth. *Nat. Rev. Cancer* **2002**, *2*, 289–300.

(3) Shinomiya, N.; Vande Woude, G. F. Suppression of Met expression: a possible cancer treatment. *Clin. Cancer Res.* **2003**, *9*, 5085–5090.

(4) Pawson, T.; Nash, P. Protein−protein interactions define specificity in signal transduction. *Genes Dev.* **2000**, *14*, 1027–1047.

(5) Peruzzi, B.; Bottaro, D. P. Targeting the c-Met signaling pathway in cancer. *Clin. Cancer Res.* **2006**, *12*, 3657–3650.

(6) http://www.vai.org/vari/metandcancer/index.as.

(7) Cui, J. J. Inhibitors targeting hepatocyte growth factor receptor and their potential therapeutic applications. *Expert Opin. Ther. Pat.* **2007**, *17*, 1035–1045.

(8) Cao, B.; Su, Y.; Oskarsson, M.; Zhao, P.; Kort, E. J.; Fisher, R. J.; Wang, L. M.; Vande Woude, G. F. Neutralizing monoclonal antibodies to hepatocyte growth factor/scatter factor (HGF/SF) display antitumor activity in animal models. *Proc. Natl. Acad. Sci. U.S.A.* **2001**, *98*, 7443–7448.

(9) (a) Schroeder, G. M.; Chen, X. T.; Williams, D. K.; Nirschl, D. S.; Cai, Z. W.; Wei, D.; Tokarski, J. S.; An, Y.; Sack, J.; Chen, Z.; Huynh, T.; Vaccaro, W.; Poss, M.; Wautlet, B.; Gullo-Brown, J.; Kellar, K.; Manne, V.; Hunt, J. T.; Wong, T. W.; Lombardo, L. J.; Fargnoli, J.; Borzilleri, R. M. Identification of pyrrolo[2,1-*f*][1,2,4]triazine-based inhibitors of Met kinase. *Bioorg. Med. Chem. Lett.* **2008**, *18*, 1945–1951. (b) Cai, Z. W.; Wei, D.; Schroeder, G. M.; Cornelius, L. A. M.; Kim, K.; Chen, X. T.; Schmidt, R. J.; Williams, D. K.; Tokarski, J. S.; An, Y.; Sack, J. S.; Manne, V.; Kamath, A.; Zhang, Y.; D'Arienzo, C.; Marathe, P.; Hunt, J. T.; Trainor, G. L.; Lombardo, L. J.; Fargnoli, J.; Borzilleri, R. M. Discovery of orally active pyrrolopyridine- and aminopyridine-based Met kinase inhibitors. *Bioorg. Med. Chem. Lett.*, **2008**, *18*, 3224–3229.

(10) Thibault, C.; L'Heureux, A.; Bhide, R.; Ruel, R. Concise and efficient synthesis of 4-fluoro-1*H*-pyrrolo[2,3-*b*]pyridine. *Org. Lett.* **2003**, *5*, 5023–5025.

(11) Houghton, R. P.; Lapham, D. J. A modified preparation of β-keto esters. *Synthesis* **1982**, *451*, 452.

(12) Baolgh, M.; Hermecz, I.; Meszaros, Z.; Simon, K.; Pusztay, L.; Horvath, G.; Dvortsak, P. Studies on chemotherapeutics I. Synthesis of 5-substituted 4-oxo-1,4-dihydro-3-pyridinecarboxylic acid derivative. *J. Heterocycl. Chem.* **1980**, *17*, 359–367.

(13) Canibano, V.; Rodriguez, J. F.; Santos, M.; San-Tejedor, M. A.; Carreno, M. C.; Gonzalez, G.; Garcia-Ruano, J. L. Mild regioselective halogenation of activated pyridines with *N*-bromosuccinimide. *Synthesis* **2001**, *2175*, 2179.

(14) Miyaura, N.; Yanagi, T.; Suzuki, A. The palladium-catalyzed cross-coupling reaction of phenylboronic acid with haloarenes in the presence of bases. *Synth. Commun.* **1981**, *11*, 513–519.

(15) Thomas, A. D.; Askan, C. V. Vilsmeier−Hack reactions of carbonyl compounds: synthesis of substituted pyrones and pyridines. *Tetrahedron* **2004**, *60*, 5069–5076.

(16) The atomic coordinates of Met Kinase complexed with **2** have been deposited in the RCSB Protein Data Bank (PDB code 3CE3).

(17) Rege-Cambrin, G.; Scaravaglio, P.; Carozzi, F.; Giordano, S.; Ponzetto, C.; Comoglio, P. M.; Saglio, G. Karyotypic analysis of gastric carcinoma cell lines carrying an amplified c-met oncogene. *Cancer Genet. Cytogenet.* **1992**, *64*, 170–173.

(18) Yokozaki, H. Molecular characteristics of eight gastric cancer cell lines established in Japan. *Pathol. Int.* **2000**, *50*, 767–777.

(19) Ponzetto, C.; Giordano, S.; Peverali, F.; Della Valle, G.; Abate, M. L.; Vaula, G.; Comoglio, P. M. c-Met is amplified but not mutated in a cell line with an activated met tyrosine kinase. *Oncogene* **1991**, *6*, 553–559.

(20) Ma, P. C.; Jagadeeswaran, R.; Jagadeesh, S.; Tretiakova, M. S.; Nallasura, V.; Fox, E. A.; Hansen, M.; Schaefer, E.; Naoki, K.; Lader, A.; Richards, W.; Sugarbaker, D.; Husain, A. N.; Christensen, J. G.; Salgia, R. Functional expression and mutations of c-Met and its therapeutic inhibition with SU11274 and small interfering RNA in non-small cell lung cancer. *Cancer Res.* **2005**, *65*, 1479–1488.

(21) Christensen, J. G.; Schreck, R.; Burrows, J.; Kuruganti, P.; Chan, E.; Le, P.; Chen, J.; Wang, X.; Ruslim, L.; Blake, R.; Lipson, K. E.; Ramphal, J.; Do, S.; Cui, J. J.; Cherrington, J. M.; Mendel, D. B. A selective small molecule inhibitor of c-Met kinase inhibits c-Met-dependent phenotypes in vitro and exhibits cytoreductive antitumor activity in vivo. *Cancer Res.* **2003**, *63*, 7345–7355.

(22) Smolen, G. A.; Sordella, R.; Muir, B.; Mohapatra, G.; Barmettler, A.; Archibald, H.; Kim, W. J.; Okimoto, R. A.; Bell, D. W.; Sgroi, D. C.; Christensen, J. G.; Settleman, J.; Haber, D. A. Amplification of MET may identify a subset of cancers with extreme sensitivity to the selective tyrosine kinase inhibitor PHA-665752. *Proc. Natl. Acad. Sci. U.S.A.* **2006**, *103*, 2316–2321.

(23) Maximum tolerated dose is defined as no more than one death in the group and/or greater than 10% weight loss.

(24) (a) Klagsbrun, M.; Moses, M. A. Molecular angiogenesis. *Chem. Biol.* **1999**, *6*, R217–R224. (b) Folkman, J.; Shing, Y. Angiogenesis. *J. Biol. Chem.* **1992**, *267*, 10931–10934. (c) Folkman, J.; Klagsbrun, M. Angiogenic factors. *Science* **1987**, *235*, 442–447.

JM800476Q